

RESEARCH

Open Access



# Tailored impact of dietary fibers on gut microbiota: a multi-omics comparison on the lean and obese microbial communities

Andrea Dell'Olio<sup>1</sup>, William T. Scott Jr.<sup>3,4</sup>, Silvia Taroncher-Ferrer<sup>5</sup>, Nadia San Onofre<sup>6,7</sup>, José Miguel Soriano<sup>5,6,8</sup> and Josep Rubert<sup>1,2\*</sup>

## Abstract

**Background** Previous studies have shown that microbial communities differ in obese and lean individuals, and dietary fiber can help reduce obesity-related conditions through diet-gut microbiota interactions. However, the mechanisms by which dietary fibers shape the gut microbiota still need to be elucidated. In this in vitro study, we examined how apple fibers affect lean and obese microbial communities on a global scale. We employed a high-throughput micro-matrix bioreactor system and a multi-omics approach to identify the key microorganisms and metabolites involved in this process.

**Results** Initially, metagenomics and metabolomics data indicated that obese and lean microbial communities had distinct starting microbial communities. We found that obese microbial community had different characteristics, including higher levels of *Ruminococcus bromii* and lower levels of *Faecalibacterium prausnitzii*, along with an increased *Firmicutes:Bacteroides* ratio. Afterward, we exposed obese and lean microbial communities to an apple as a representative complex food matrix, apple pectin as a soluble fiber, and cellulose as an insoluble fiber. Dietary fibers, particularly apple pectin, reduced *Acidaminococcus intestini* and boosted *Megasphaera* and *Akkermansia* in the obese microbial community. Additionally, these fibers altered the production of metabolites, increasing beneficial indole microbial metabolites. Our results underscored the ability of apple and apple pectin to shape the obese gut microbiota.

**Conclusion** We found that the obese microbial community had higher branched-chain amino acid catabolism and hexanoic acid production, potentially impacting energy balance. Apple dietary fibers, especially pectin, influenced the obese microbial community, altering both species and metabolites. Notably, the apple pectin feeding condition affected species like *Klebsiella pneumoniae* and *Bifidobacterium longum*. By using genome-scale metabolic modeling, we discovered a mutualistic cross-feeding relationship between *Megasphaera sp.* MJR8396C and *Bifidobacterium adolescentis*. This in vitro study suggests that incorporating apple fibers into the diets of obese individuals can help modify the composition of gut bacteria and improve metabolic health. This personalized approach could help mitigate the effects of obesity.

**Keywords** Gut microbiota, Metagenomics, Metabolomics, Gut microbial metabolites, Pectin, Obese, Metabolic modelling

\*Correspondence:

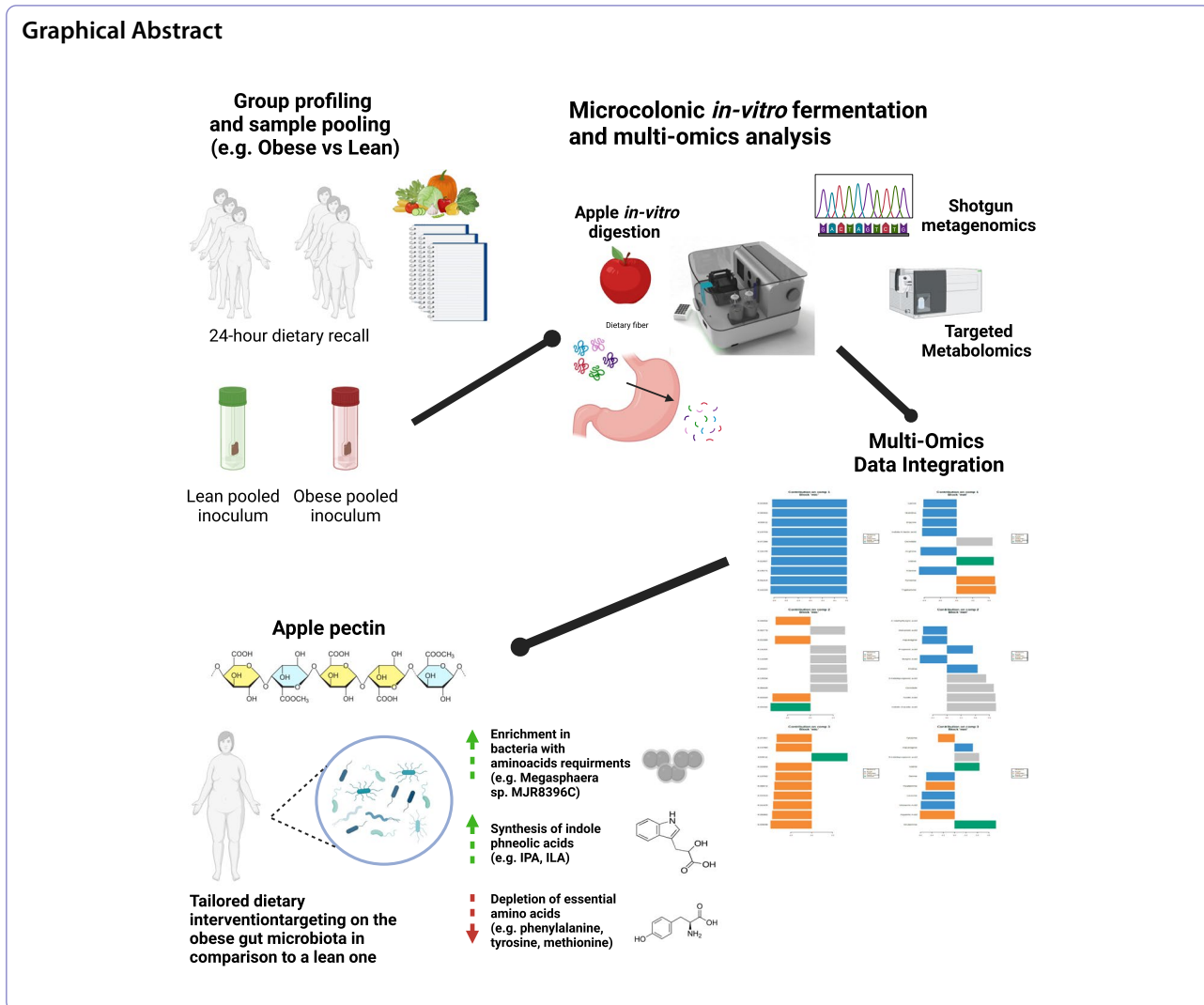
José Rubert

josep.rubert@wur.nl

Full list of author information is available at the end of the article



© The Author(s) 2024. **Open Access** This article is licensed under a Creative Commons Attribution-NonCommercial-NoDerivatives 4.0 International License, which permits any non-commercial use, sharing, distribution and reproduction in any medium or format, as long as you give appropriate credit to the original author(s) and the source, provide a link to the Creative Commons licence, and indicate if you modified the licensed material. You do not have permission under this licence to share adapted material derived from this article or parts of it. The images or other third party material in this article are included in the article's Creative Commons licence, unless indicated otherwise in a credit line to the material. If material is not included in the article's Creative Commons licence and your intended use is not permitted by statutory regulation or exceeds the permitted use, you will need to obtain permission directly from the copyright holder. To view a copy of this licence, visit <http://creativecommons.org/licenses/by-nc-nd/4.0/>.



## Introduction

The gut microbiome is a complex and diverse community of microorganisms that plays a crucial role in human health and disease [1–3]. Various factors, including diet, lifestyle, transit time, and host genetics, influence the composition and functionality of the gut microbiome [4] and consequently have an impact on the host’s health [5, 6]. Dietary habits are significantly influential on the composition and functionality of the gut microbiome [6, 7]. During the last decade, nutritional interventions, including the consumption of dietary fibers, have claimed to induce changes in the microbial landscape and its functionality in health and disease [6–9], underscoring the pivotal role of diet in promoting metabolic health [4, 7, 9]. However, the notion of a “one diet fits all” approach is often criticized because individual responses to diets can vary greatly based on genetic, metabolic, and lifestyle factors. Research on healthy subjects to prevent

diseases is as important as overcoming multifaceted and global challenges, such as obesity, that may lead to non-communicable diseases. This research is vital for creating a healthier future and mitigating the widespread impact of obesity. In this frame, extensive research over recent years has linked an altered gut microbiome and obesity [10, 11], suggesting that the gut microbiota composition and gut microbial metabolites (GMMs) might play a critical role in modulating the pathophysiology of this condition [12, 13]. However, understanding the connection between diet and the gut microbiome is absolutely crucial in tackling obesity and its underlying mechanisms [14]. At the microbial level, several research works have documented substantial differences in the gut microbial diversity, composition, and metabolic functions between lean and obese individuals [10, 15]. These differences include variations in the abundance of certain bacterial phyla, such as *Firmicutes* and *Bacteroidetes*, which play

a profound role in the modulation of host metabolism [11, 16]. In particular, an imbalance favoring *Firmicutes* over *Bacteroidetes* in obese individuals has been linked to increased production of metabolic endotoxins, such as lipopolysaccharides (LPS), which can also contribute to the obesity-related metabolic dysregulation [17]. Although diet is considered one of the main contributors to gut dysbiosis in obesity [8, 9, 14, 18], it is unclear whether compromised microbial communities can utilize undigested food as effectively as a richer and more diverse gut microbiota that is commonly found in healthy subjects. Recent research has revealed a broader impact of dietary fibers on the gut microbiota, which extends beyond short-chain fatty acids (SCFAs) modulation [18–22]. For instance, Huang et al. highlighted how fiber supplementation can affect the composition of the gut microbiota and the microbial catabolism of tryptophan depending on the colon segment [20, 21]. Evidence indicates that dietary fibers may protect against obesity by reshaping the gut microbiota and its metabolic landscape [22, 23]. However, the mechanisms remain elusive. In a recent study, Li et al. demonstrated how resistant starch induced changes in the gut microbiota, altering the global bile acid profile, reducing inflammation by restoring the intestinal barrier, and inhibiting lipid absorption [23]. However, the effect of dietary fibers has shown to have different impacts on individuals [24, 25]. In vitro, a few studies pointed out how the same dietary fiber differently modulated lean and obese microbial communities [8, 26]. Therefore, there is a need for designing dietary interventions tailored to the targeted gut microbiota [7, 24, 27]. In other words, personalizing the diet based on individual needs and health conditions is essential for maximizing its effectiveness. Our study aimed to investigate the impact of dietary fibers on the behavior of GMMs, as well as the composition and function of microbial communities in both lean and obese microbial communities. We suspected that impaired microbial communities may not effectively use and prioritize dietary fibers, unlike more diverse and functional microbial communities. To this end, we collected stools from individuals clinically characterized as healthy lean or healthy obese subjects. By utilizing the INFOGEST in vitro digestion protocol and a micro-matrix bioreactor for reproducible batch cultures of colon fermentation, we simulated the digestion of apple, apple pectin, and cellulose and their subsequent colonic fermentation by the lean and obese microbial communities [26, 28, 29]. A multi-omics approach, integrating shallow shotgun metagenomics and targeted metabolomics (amino acids, SCFAs, and tryptophan-related metabolites), provided a comprehensive view of how dietary fibers distinctly modulated microbial composition and function in lean and obese

microbial communities. *Megasphaera* spp. *MJR8396C* showed enrichment in the presence of soluble fibers in the obese microbial community, and we employed genome-scale metabolic modeling to ultimately study amino acid metabolism. This approach deepens our comprehension of a representative obese microbial community and the impact of specific dietary fibers on shaping the gut microbiota of obese individuals compared to lean ones. In addition, we provided a valuable in vitro strategy to study food - gut microbiota interactions and expand our understanding of how dietary compounds could be used as therapeutic and preventive tools.

## Methods

### Recruitment

The study was conducted from November to December 2021. It was approved by the Biomedical Research Ethics Committee (2018-026 - University of Trento), respecting the fundamental principles of the Declaration of Helsinki, the Council of Europe Convention in relation to Human Rights and Biomedicine, and the UNESCO Declaration. Six patients (four males and two females) were recruited by the Clinic of Nutrition, Physical Activity, and Physiotherapy, Lluís Alcanyis Foundation (University of Valencia). The mean age of participants was 34.8  $\pm$  8.6 years. To each participant, we explained the nature and purpose of the study, obtaining voluntarily informed consent from all of them. For anthropometrical assessment, participants were instructed to wear light clothing. They were positioned in accordance with the manufacturers' recommendations being height measured in a standing position and after a normal expiration using a stadiometer (SECA 225, range, 60/200 cm; the precision of 1 mm, Hamburg, Germany) and weight, body mass index (BMI) ( $\text{kg}/\text{m}^2$ ), basal metabolic rate (kcal), fat mass (kg), body fat (%), muscle mass (kg), bone mineral mass (kg), fat-free mass (kg), total body water (kg), and their percentages (%) obtained using multi-frequency segmental body composition analyzer (Tanita MC780MA; Tanita Corporation, Tokyo, Japan) [30]. Twenty-four hours before the measurements were carried out, the participants were advised to refrain from vigorous exercise, not consume any alcohol drinks, to avoid energetic drinks, and to be fasting for at least 8 h, according to [31]. For dietary consumption, the EFSA Guidance Document compiled by the EFSA Expert Group on Food Consumption Data [32], recommends that surveys cover two non-consecutive days and that the 24-h recalls must be used for adults. The 24-h recall interview, repeated at least once and not conducted on consecutive days, was selected as the most suitable method to get population means and distributions [33]. Estimation of portion sizes, interviewed by nutritionists/dieticians, with a picture book, including

country-specific dishes, with additional household and other relevant measurements. Daily energy, macronutrient (protein, carbohydrates, and lipids), micronutrient (vitamins and minerals), and some bioactive compounds consumption was calculated using the DIAL program (Department of Nutrition UCM, Alce Ingenieria S. L., Madrid, Spain) [34].

### **In vitro digestion and batch fermentation**

Dietary fibers (apple pectin and cellulose) and a food model (an apple, Renetta Canada variety) were digested following the protocol reported by Brodkorb et al. [28]. Briefly, the apple, apple pectin, and cellulose underwent simulated oral, gastric, and intestinal digestion under specific conditions (i.e., temperature, electrolytes, pH, and enzymes). After the intestinal phase, the digesta was centrifuged at 4500 g for 20 min to separate the bioaccessible (supernatant) and undigested fractions (pellet). The latter was used as the starting material to perform the colonic fermentation. Fecal samples were collected from obese individuals with body mass index (BMI) greater than 30 (kg/m<sup>2</sup>) and lean (BMI lower than 25 kg/m<sup>2</sup>) individuals. Stool samples were collected using sterile and anaerobic containers and transported to the laboratory on ice within 2 h of collection. The fecal samples from obese ( $n = 3$ ) and lean ( $n = 3$ ) volunteers were pooled to obtain the fecal inoculum for each class [26]. The micro-Matrix (Applikon Biotechnology, Heertjeslaan 2, 2629 JG Delft, Netherlands) was used to model the human distal colon. The fermentations were conducted in sealed micro-Matrix cassettes (24 wells/cassette). The mini-bioreactor settings were based on O'Donnell and co-authors [29], with a pH adjusted at 6.8. The experiment was conducted under-regulated pH (6.8), N<sub>2</sub> flow (full anaerobic environment), and temperature control at 37 °C. The medium was composed of peptone water, yeast extract, bile salts, cysteine, vitamin K, and several salts, as described elsewhere [35]. The inoculum was then divided into equal portions and exposed to control (medium), apple, apple pectin, and cellulose at a concentration of 2% (w/v). Several fermentations were conducted in parallel using 5 ml, and experiments were conducted in triplicates. Samples were withdrawn at time 0 and after 24 h for DNA extraction and targeted metabolomics. All samples were stored at -80 °C for further analysis.

### **Targeted metabolomics analysis**

The slurries were collected and centrifuged at 5 °C, 12,500 g, for 10 min to remove any particulate matter [20, 21, 36, 37]. SCFAs, amino acids, branched-chain amino acids (BCAAs), branched-chain fatty acids (BCFAs), and tryptophan-related metabolites were analyzed using methods previously developed by our group [20, 21, 36,

37]. Briefly, SCFAs were extracted and analyzed using the method described by Lotti et al. [36]. The remaining metabolites were extracted and quantified as Huang et al. described [20, 21, 37]. For the liquid chromatography-mass spectrometry (LC-MS) analyses, supernatants were filtered and diluted 10-fold with Milli-Q water before being injected. By LC-MS, we monitored indole-3-propionic acid (IPA), indole-3-acetic acid (IAA), indole-3-lactic acid (ILA), indole (Ind), oxindole (Oxi), indoleacrylic acid (IA), indole-3-aldehyde (I3A), tryptamine (TA), kynurenine (Kyn), serotonin (5-HT), and amino acids.

### **Metagenomics analysis**

A total of 1 ng of DNA was used following the manufacturer's instructions for the Nextera XT Library kit (Illumina). DNA was simultaneously fragmented and tagged with dual index sequencing adapters that enable accurate assignment of reads per sample. Library quality control was ensured by profiling and length distribution analysis using the HSD5000 kit in the TapeStation 4200 equipment (Agilent). The NovaSeq 6000 sequencing platform in a 150 paired-end reads configuration generated \*.bcl files as primary sequencing output (NovaSeq Control Software (NCS) version 1.6). The Bcl2fastq 2.20 program was used to translate the sequencing reads from bcl (Base Calling) to FASTQ format. This step also removed sequencing adapters. The Clumpify tool from the BBTools suite was used to remove optical duplicates [38]. Reads with a Phred quality score less than Q20 and a length of less than 50 nucleotides were filtered out using the program BBDump v38.36 [38]. The presence of the human genome was filtered using NGLess v1.0.0-Linux64 [39]. The Homo sapiens hg19 genome, which is built-in in NGLess, was used. We then aligned the sequences to the genomes, and those with alignments of more than 45 bases and 97% similarity were discarded. The remaining sequences were called "High Quality sequences" and were meant to be the final sequences. This resulted in the generation of around 400 million raw reads and approximately 120 gigabases of sequence data. The metagenomic data were subjected to analysis utilizing bioBakery processes, including all essential dependencies and employing default values as described [40]. In this study, KneadData 0.7.10 was used for the purpose of trimming and filtering the raw sequence reads. The taxonomic profiling of samples that successfully passed quality control was conducted at the species level using MetaPhlan v3.0. This software utilizes alignment to a reference database of "marker genes" to determine the taxonomic composition of the samples [41]. The collection of raw sequences and related metadata were deposited at NCBI with the bioproject ID 1089942.

### Bioinformatics and statistical analysis

The metagenomics data tables were merged with the metadata, split per time points using *tidyverse* in R. The generated datasets were analyzed using *MicrobiomeAnalyst*, an online statistical, functional and integrative analysis of microbiome data in R [42]. The following subsections describe the specific tools used for the metagenomics and metabolomics datasets.

#### **Principal coordinate analysis (PCoA) on metagenomics data**

To assess the dissimilarity between donors and pooled samples, a non-metric multidimensional scaling was performed in *Microbiome Analyst 2.0* [42]. To assess beta-diversity between the before and after intervention a principal coordinate analysis (PCoA) was performed. We used PERMANOVA to test whether two or more groups of samples were significantly different based on categorical variables.

#### **Identification of significant features using multi-factory analysis**

To identify significant taxonomic and metabolic features between the studied conditions we used *MaAsLin2* (*Microbiome Multivariable Association with Linear Models*) and *Limma* (*Linear Models for Microarray Data*) [43, 44]. These tools use general linear models to find associations between microbial features and experimental metadata [43, 44]. We used an adjusted *p*-value cut-off of 0.05 and an absolute log fold change of 2 to select significant metabolites, KOs, and species. Comparisons were conducted at both baseline (time zero) and after 24 h of fermentation. At baseline, we found no statistically significant differences between the control and the medium supplemented with apple, apple pectin, and cellulose, indicating comparable starting conditions. After 24 h, this analysis enabled us to evaluate the time-dependent effects of feeding conditions on the lean and obese microbial communities.

#### **Genome-scale metabolic modeling reconstruction and genome mining**

##### ***GutSMASH***

*GutSMASH* was used to predict the metabolic gene clusters (MGCs) that are responsible for the synthesis of primary metabolites in gut anaerobic bacteria [45, 46]. The *Megasphaera* sp. MJR8396C *GutSMASH* results were generated using the assembly GCA001546855.1 on NCBI.

##### ***Genome-scale metabolic reconstruction***

The genome sequences of *Megasphaera* sp. MJR8396C and *Bifidobacterium adolescentis* ATCC 15703 were obtained from the National Center for Biotechnology

Information (NCBI) database. Prior to metabolic model reconstruction, the genome sequences underwent quality assessment and preprocessing to ensure accuracy and completeness. The genome-scale metabolic models (GSMMs) for both *Megasphaera* sp. MJR8396C and *Bifidobacterium adolescentis* ATCC 15703 were reconstructed using *gapseq* [47], a comprehensive tool designed for the automated reconstruction of metabolic models from genomic data. *gapseq* integrates genomic annotation with metabolic pathway databases to predict the metabolic capabilities of an organism based on its genome sequence. The process began with the annotation of the genomes using *gapseq*'s built-in functional annotation tools, which identify genes involved in metabolic processes and assign them to specific reactions and pathways. Following annotation, *gapseq* performed a draft reconstruction of the metabolic network for each organism. This draft model included predicted metabolic reactions, associated genes, and metabolic pathways present in the organism's genome. The draft models were then subjected to a gap-filling process to resolve missing reactions and pathways that are essential for a functional metabolic network but were not directly evident from the genomic data. The gap-filling process was conducted using a synthetic human gut-like medium, designed to mimic the nutrient composition and availability found in the human gastrointestinal tract. This approach allowed for the identification and addition of metabolic reactions necessary for growth and survival in a gut-like environment, thereby enhancing the biological relevance and accuracy of the reconstructed models. The synthetic medium composition was based on known concentrations of carbohydrates, amino acids, fatty acids, vitamins, and minerals typical of the human gut environment. By simulating growth in this medium, gaps in the metabolic network were identified where essential nutrients could not be synthesized or metabolized by the organism under study. These gaps were filled by adding reactions that enabled the utilization or synthesis of the missing components, ensuring the model's capability to simulate growth in a gut-like environment. The final step in the reconstruction process involved the refinement and checks of the metabolic models. This included the verification of model predictions, where available. The models were assessed for their ability to predict growth rates, substrate utilization profiles, and metabolic product formation under anaerobic fermentative conditions similar to those in the human gut. To assess the metabolic potential of the models, parsimonious Flux Balance Analysis (pFBA) and Flux Variability Analysis (FVA) were performed. Parsimonious Flux Balance Analysis (pFBA) aims to minimize the total flux of all reactions in the model while satisfying the same constraints as standard

FBA, thus representing a more efficient metabolic state that cells might prefer under certain conditions. The optimization problem for pFBA can be formulated as follows:

$$\min \sum_j |v_j| \quad (1)$$

subject to:

$$S \cdot v = 0 \quad (2)$$

$$v_{\min} \leq v \leq v_{\max} \quad (3)$$

$$\max \left\{ c^T \cdot v \right\} \text{ (from FBA)} \quad (4)$$

where  $v_j$  represents the flux through reaction  $j$ ,  $S$  is the stoichiometric matrix,  $v$  is the vector of all reaction fluxes,  $v_{\min}$  and  $v_{\max}$  are the lower and upper bounds on fluxes, respectively, and  $c^T \cdot v$  is the objective function (e.g., biomass production) maximized in the initial FBA step. Flux Variability Analysis (FVA) is used to determine the range of possible fluxes through each reaction in the model under a given set of constraints, providing insights into the flexibility of metabolic networks. The FVA problem for each reaction can be described by the following pair of optimizations:

$$\max/\min v_j \quad (5)$$

Subject to:

$$S \cdot v = 0 \quad (6)$$

$$v_{\min} \leq v \leq v_{\max} \quad (7)$$

$$c^T \cdot v = \text{fixed objective value} \quad (8)$$

Where the conditions are the same as those for pFBA, but the objective is to find the maximum and minimum allowable fluxes through each reaction  $j$  while maintaining a fixed objective value (usually the optimal biomass production rate found by FBA). These analyses provided a comprehensive assessment of the metabolic capabilities and flexibility of the reconstructed models of *Megasphaera* sp. MJR8396C and *Bifidobacterium adolescentis* ATCC 15703, under conditions mimicking the anaerobic fermentative environment of the human gut.

#### Genome-scale metabolic modelling analysis in co-culture simulations using BacArena

Genome-scale metabolic modeling analysis of the co-culture comprising *Megasphaera* sp. MJR8396C and *Bifidobacterium adolescentis* ATCC 15703 was conducted using BacArena [48], a spatial dynamic Flux Balance Analysis (dFBA) metabolic modeling approach. Since

we did not have information on the specific strain of *Bifidobacterium adolescentis*, we decided to reconstruct the reference genome ATCC 15703 from AGORA [49]. BacArena enables the simulation of interactions between multiple microbial species within a defined environment, accounting for spatial distribution and nutrient availability. For implementing this approach, we followed a structured tutorial available at <https://bacarena.github.io/>, which provided step-by-step guidance on setting up and running co-culture simulations. A prerequisite for conducting simulations with BacArena is a working installation of R and the Sybil package, which facilitates the integration of GEMs into the simulation environment. In this study, we utilized R version 2023.12.0+369 and Sybil version 2.2.0. The GEMs of *Megasphaera* sp. MJR8396C and *Bifidobacterium adolescentis* ATCC 15703 were incorporated into BacArena to simulate metabolic exchanges between these microbial species. Simulations were carried out on a  $20 \times 20$  grid environment over a period of 24 h, providing a detailed spatial and temporal resolution of microbial interactions and metabolic dynamics. The environment was initialized with a synthetic gut medium, as described by Zimmermann et al. [48], to mimic the nutrient composition found in the human gastrointestinal tract. This setup ensured that the simulations reflected realistic conditions conducive to the growth and interaction of gut microbiota. The initial amounts and biomasses of both species were set at a ratio of 1:1 to simulate an equimolar starting concentration of each microbe. This setup aimed to explore the dynamics of competition and cooperation between the species under balanced initial conditions. Furthermore, the diffusion of metabolites within the simulation environment was calibrated based on the standard diffusion rate of glucose, ensuring that nutrient transport and availability were realistically modeled.

## Results

### Participant grouping and metagenomics analyses

Comparative analyses of anthropometric and diet variables were conducted by dividing the six participants into two groups based on BMI, where obese participants had a  $\text{BMI} \geq 30$  and lean participants had a  $\text{BMI}$  within  $19 \leq \text{BMI} \leq 24.9$  as described by the Global Health Observatory data repository [50]. The analysis of variance (ANOVA) was utilized to determine the statistical significance of differences between groups, denoted by the  $F$ -statistic, where  $F(\text{df}_{\text{between}}, \text{df}_{\text{within}})$  describes the ratio of the variance calculated between the groups to the variance within the groups. The fat mass demonstrated statistically significant differences between groups, with the obese group showing higher values (mean = 34.47, SD = 0.71) than the lean group (mean = 12.60, SD = 0.70),  $F(1,$

4) = 1444.081,  $p \leq 0.001$ . Protein intake was also significantly higher in obese subjects (mean = 10.87, SD = 2.12) compared to the lean group (mean = 16.13, SD = 2.25),  $F(1, 4) = 8.698$ ,  $p \leq 0.05$ . The intake of soluble fibers was significantly higher in the obese group (mean = 4.40, SD = 0.66) compared to the lean group (mean = 2.20, SD = 0.17),  $F(1, 4) = 31.565$ ,  $p = 0.005$ . Saturated fatty acids (SFA) intake differed significantly, with the obese group consuming more (mean = 49.27, SD = 6.95) than the lean group (mean = 26.40, SD = 7.95),  $F(1, 4) = 14.064$ ,  $p = 0.020$ . Similarly, monounsaturated fatty acids (MUFA) intake was higher in the obese group (mean = 47.03, SD = 11.82) compared to the lean group (mean = 21.37, SD = 9.23),  $F(1, 4) = 8.791$ ,  $p = 0.041$ . Iron intake showed a significant difference, being higher in the obese group (mean = 15.77, SD = 2.29) versus the lean group (mean = 10.23, SD = 1.46),  $F(1, 4) = 12.503$ ,  $p = 0.024$ . Within each group, there were no statistically significant differences, indicating that subjects within the same group could be considered homogeneous in terms of diet and anthropometric values. The full anthropometric data and statistical test results are provided in Supplementary Data S1, S2, and S3. Data S1 provides a general overview of the acquired data, Data S2 compares the obese versus lean groups, and Data S3 includes statistics comparisons by gender. Having established the uniformity within groups and established the main distinct features between groups, we next directed our analysis toward examining the gut microbiota compositions of the individual donors and the pooled samples. Figure 1A illustrates the microbial composition at the species level of the top 20 most abundant species in obese and lean donors, highlighting the differences in species distribution between the two groups. Each vertical bar represents a sample from a specific donor, with different colors indicating the relative abundance of specific bacterial species. Lean donors' samples consistently showed a higher relative abundance of *Faecalibacterium prausnitzii*. Additionally, species such as *Bifidobacterium longum* and *Bifidobacterium adolescentis* were more prominent in lean samples compared to obese donors. Within the lean donors, while all exhibit high levels of *Faecalibacterium prausnitzii*, there were variations in the relative abundance of other species like *Bifidobacterium longum* and *Eubacterium hallii*. Donor 1 showed a higher abundance of *Bifidobacterium bifidum* compared to Donors 2 and 3. In contrast, samples from obese donors were characterized by a higher relative abundance of *Ruminococcus bromii*. There was also a noticeable presence of species such as *Alistipes inops* and *Coprococcus catus* in obese donors. The relative abundance of different bacterial species showed significant variability. For instance, donor 1 had a higher relative abundance of *Alistipes inops* compared to

donors 2 and 3. Donor 3 exhibited a more diverse bacterial profile with significant proportions of *Coprococcus comes* and *Roseburia faecis* compared to other obese donors. Overall, this figure highlights clear differences in the gut microbiota composition between lean and obese donors, with specific bacterial species being more predominant in each group. The intra-group variability also suggested individual differences in the gut microbiota composition within both the lean and obese categories. In Fig. 1B, we show the microbial composition at the species level of the top 20 most abundant species in the pooled samples, from now on called microbial community. The lean microbial community exhibited a consistently higher relative abundance of *Faecalibacterium prausnitzii*. Additionally, species such as *Bifidobacterium longum* and *Bifidobacterium adolescentis* were more prominent in the lean microbial community compared to the obese one. By contrast, the obese microbial community was characterized by a higher relative abundance of *Ruminococcus bromii*. There was also a noticeable presence of species such as *Alistipes inops* and *Coprococcus catus* in the obese microbial community. Furthermore, at the phylum level, the obese microbial community showed a statistically significant higher *Firmicutes:Bacteroidetes* ratio ( $p \leq 0.01$ ), as shown in Supplementary Figure S1. Overall, pooling reduced the within-group variation, producing a representative profile of both lean and obese gut microbiota. The consistency in preserving key species, such as *Ruminococcus Bromii* in the obese and *Faecalibacterium Prausnitzii* in lean, and keeping the *Firmicutes:Bacteroidetes* ratio suggested that the pooling process did not drastically alter the microbial community, making it a reliable method to study the effect of dietary fibers on fully characterized microbial communities. To further assess the effects of the pooling process, we employed non-metric multidimensional scaling (NMDS), as shown in Fig. 1C. This analysis was used to assess differences between individual donors and pooled samples (microbial communities), yielding an  $R$ -squared value of 0.33824 and a  $p$ -value of 0.26. Pooled samples closely clustered together, suggesting that the pooling procedure resulted in a consistent and homogeneous inoculum. This clustering implies that the individual variability among donors was effectively minimized, providing a more stable baseline for evaluating the effects of dietary fibers. After assessing the composition of the microbial communities, we analyzed the microbial composition at the species level of the top 20 most abundant species at  $t = 0$  h (Fig. 1D) and  $t = 24$  h (Fig. 1E) across various feeding conditions (apple, apple pectin, cellulose, and control). The baseline data in Fig. 1D was crucial for understanding the initial condition of each feeding regimen and allowed for a more precise evaluation of how

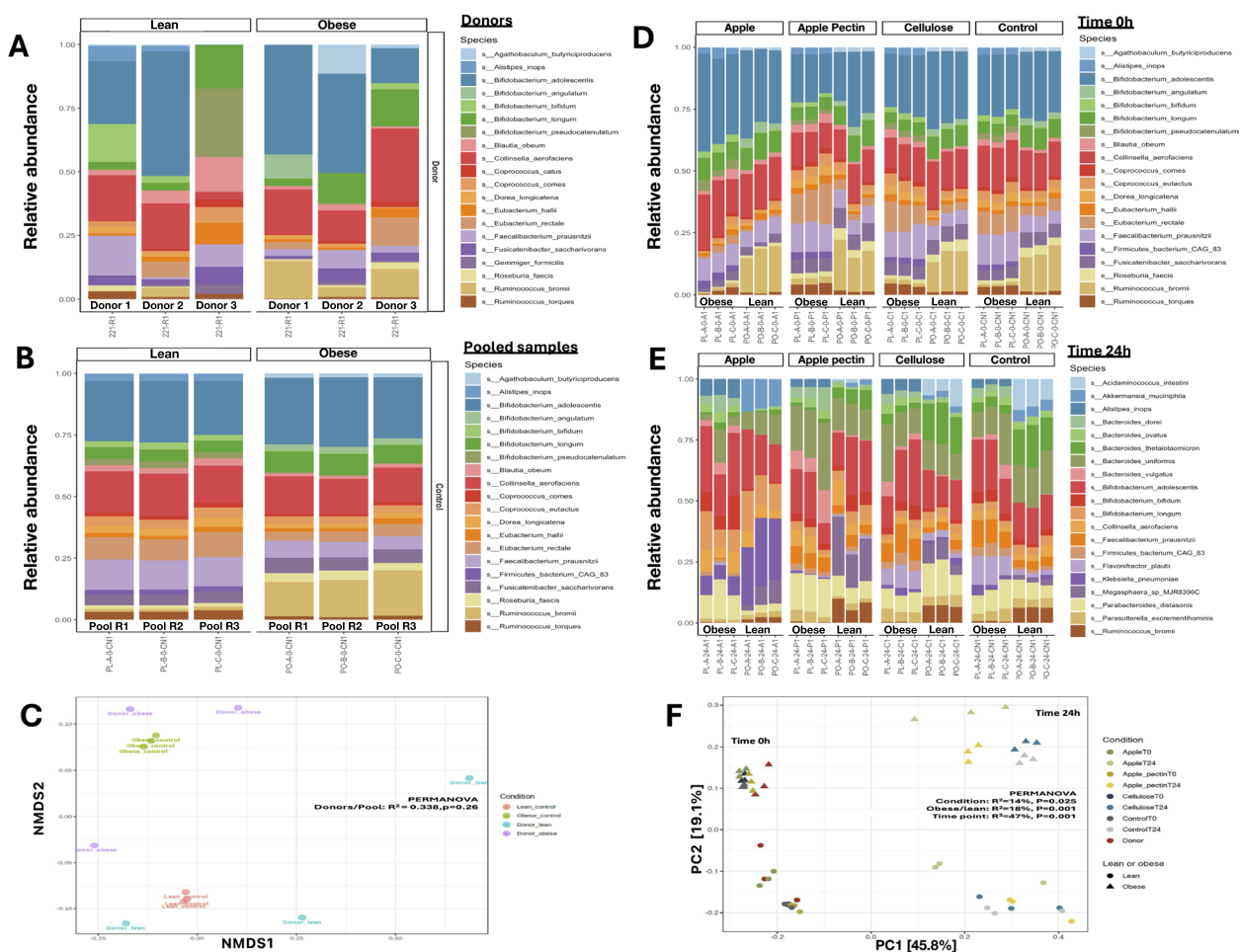


**Fig. 1** **A** Microbial composition at the species level of the top 20 most abundant species in obese and lean donors, highlighting the differences in species distribution between the two groups. **B** Microbial composition at the species level of the top 20 most abundant species in pooled fecal samples from lean and obese donors, illustrating the integration and overall community structure in pooled samples. **C** NMDS plot displaying microbial community structure at the species level for individual donors (donor 1, donor 2, donor 3) and pooled samples (pool R1, pool R2, pool R3) at two time points (0 h and 24 h). PERMANOVA analysis indicates no significant change due to the pooling process ( $R^2 = 0.338, p = 0.26$ ). **D** Microbial composition at the species level of the top 20 most abundant species at 0 h across various feeding conditions and controls, demonstrating the initial community structure. **E** Microbial composition at the species level of the top 20 most abundant species after 24 h exposed to the feeding conditions, showing the effects of different dietary fibers over time. **F** The NMDS plot shows significant differences between lean and obese samples under various feeding conditions. PERMANOVA analysis reveals the effects of feeding conditions ( $R^2 = 14\%, p = 0.025$ ), obesity status ( $R^2 = 18\%, p = 0.001$ ), and time points ( $R^2 = 47\%, p = 0.001$ ) on the composition of microbial communities. Data are representative of three independent fermentation experiments ( $n = 3$ ) using pooled fecal inoculum from either lean or obese groups

different dietary fibers affect microbial composition over time. On the other hand, Fig. 1E revealed the dynamic changes in the microbial community due to the dietary fiber supplementation. Significant changes in the microbial composition were evident across the feeding conditions. Apple feeding condition led to an increase in the relative abundance of *Bacteroides* species in both lean and obese microbial communities. In the lean microbial community, the microbial profile became more balanced, while in the obese microbial community, although *Ruminococcus bromii* remained prominent, the overall

diversity increased. Apple pectin feeding condition resulted in a notable increase in *Bifidobacterium* species in both lean and obese microbial communities. Nevertheless, the lean microbial community continued to show higher levels of *Faecalibacterium prausnitzii*. The cellulose feeding condition also led to an increase in *Bacteroides*, particularly in the lean microbial community. On the contrary, the obese microbial community showed a moderate increase in these species, with *Ruminococcus bromii* still maintaining a significant presence. This suggests that cellulose, an insoluble fiber, while beneficial,



may not be as effective as apple pectin in altering the obese microbial community. In controls, where no fiber was added, the changes in microbial composition were less pronounced. However, there was still an observable shift towards an increased presence of *Bacteroides* species in both lean and obese microbial communities, indicating some baseline microbial activity and adaptation. These results emphasize the potential of dietary fibers, such as apple and apple pectin, to beneficially modulate the gut microbiota composition. Apple pectin, in particular, showed a strong effect in increasing the abundance of beneficial bacterial species. In Fig. 1F, we present a PERMANOVA analysis to evaluate the impact of feeding conditions (fibers and control), obesity versus lean, and time on microbial community composition. The results indicated that the microbial composition was significantly different between obese and lean samples, with feeding conditions ( $R^2 = 14\%$ ,  $p = 0.025$ ), obesity status ( $R^2 = 18\%$ ,  $p = 0.001$ ), and time points ( $R^2 = 47\%$ ,  $p = 0.001$ ) all having significant effects. These findings highlight the substantial impact of dietary fibers on microbial communities, which varies based on the initial microbial composition. Overall, results suggest that in vitro short-term interventions had a distinct effect on lean and obese microbial communities.

#### **Obese and lean microbial communities have distinct metabolic signatures for BCAA and BCFA**

The targeted metabolomics analysis revealed notable distinctions in metabolic profiles between lean and obese microbial communities, particularly regarding the final concentrations of BCAAs and BCFAs. Supplementary Figure S2 and Fig. 2A illustrate the initial and final concentration of BCAAs (leucine, isoleucine, valine) and BCFAs (isovaleric acid, 2-methylbutyric acid, isobutyric acid) measured in millimolars (mM) across the various dietary treatments for both lean and obese microbial communities. Under apple feeding conditions, the lean microbial community yielded mean concentrations of  $42.35 \pm 3.82$  mM for leucine,  $13.36 \pm 0.87$  mM for isoleucine, and  $86.30 \pm 6.62$  mM for valine. Conversely, in the obese microbial community, the mean concentrations under the same feeding condition were notably lower. For instance, in the lean microbial community exposed to cellulose, mean concentrations of leucine, isoleucine, and valine were  $31.46 \pm 9.70$ ,  $8.73 \pm 1.73$  mM, and  $69.85 \pm 17.39$  mM, respectively. In contrast, obese exhibited lower concentrations under the same conditions ( $0.80 \pm 0.48$  mM for leucine,  $0.26 \pm 0.30$  mM for isoleucine, and  $6.32 \pm 1.56$  mM for valine). Interestingly, the control groups that did not receive dietary fiber treatment showed similar trends of BCAA concentrations. This suggests that the distinctive metabolic signature of BCAAs is

not a result of the feeding conditions but rather a signature that sets apart lean and obese microbial communities. Regarding BCFAs, Fig. 2B illustrates how the obese microbial community consistently exhibited elevated concentrations compared to their lean counterpart across all feeding conditions and the control. For instance, under apple feeding conditions, the obese microbial community had a mean concentration of isovaleric acid at  $2664.11 \pm 78.18$  mM. In comparison, the lean microbial community exhibited a markedly lower concentration of  $338.62 \pm 64.31$  mM. This pattern persisted across the other BCFAs and feeding conditions, emphasizing the heightened metabolic activity for BCFA synthesis in the obese microbial community. Overall, these findings underscore a significant disparity in BCAA and BCFA concentrations between lean and obese microbial communities, indicating a distinct metabolic potential across the two microbial communities. The full dataset, including the concentration before and after treatments for BCAAs and BCFAs and Tukey's multiple comparisons, are presented in Supplementary Data S7, S8, and S9. As illustrated in Fig. 3, another striking difference between the lean and obese microbial communities was the final concentrations of hexanoic acid (HA) and butyric acid (BA). Specifically, in Fig. 3A and B, we observed varying concentrations of BA across different feeding conditions. At the same time, for HA, the variation between lean and obese microbial communities was again irrespective of the feeding conditions. As an example, in the lean microbial community exposed to the apple feeding condition, BA exhibited a mean concentration of  $1095.81 \pm 794.04$  mM, while HA showed a mean concentration of  $25.20 \pm 0.92$  mM. In contrast, in the obese microbial community under the same apple feeding condition, BA showed a mean concentration of  $1859.31 \pm 263.49$  mM, while HA exhibited a higher mean concentration of  $266.66 \pm 26.01$  mM. Notably, the apple pectin feeding condition in the lean microbial community induced the highest concentration of BA ( $3235.80 \pm 211.19$  mM) among all feeding conditions. These findings collectively underscore that the obese microbial community showed a consistently higher concentration of HA independently of the feeding conditions. By contrast, BA concentrations in both lean and obese microbial communities were regulated by our feeding conditions. To identify a potential biomarker capable of differentiating between lean and obese microbial communities and physiological states, we performed a comparison of the log ratio of BA/HA. In Fig. 3C, a significant difference in the log BA/HA ratio was observed between lean and obese microbial communities across all the studied conditions. This ratio was significantly higher ( $p \leq 0.001$ ) in the lean microbial community compared to the obese one, suggesting a possible predictive ability

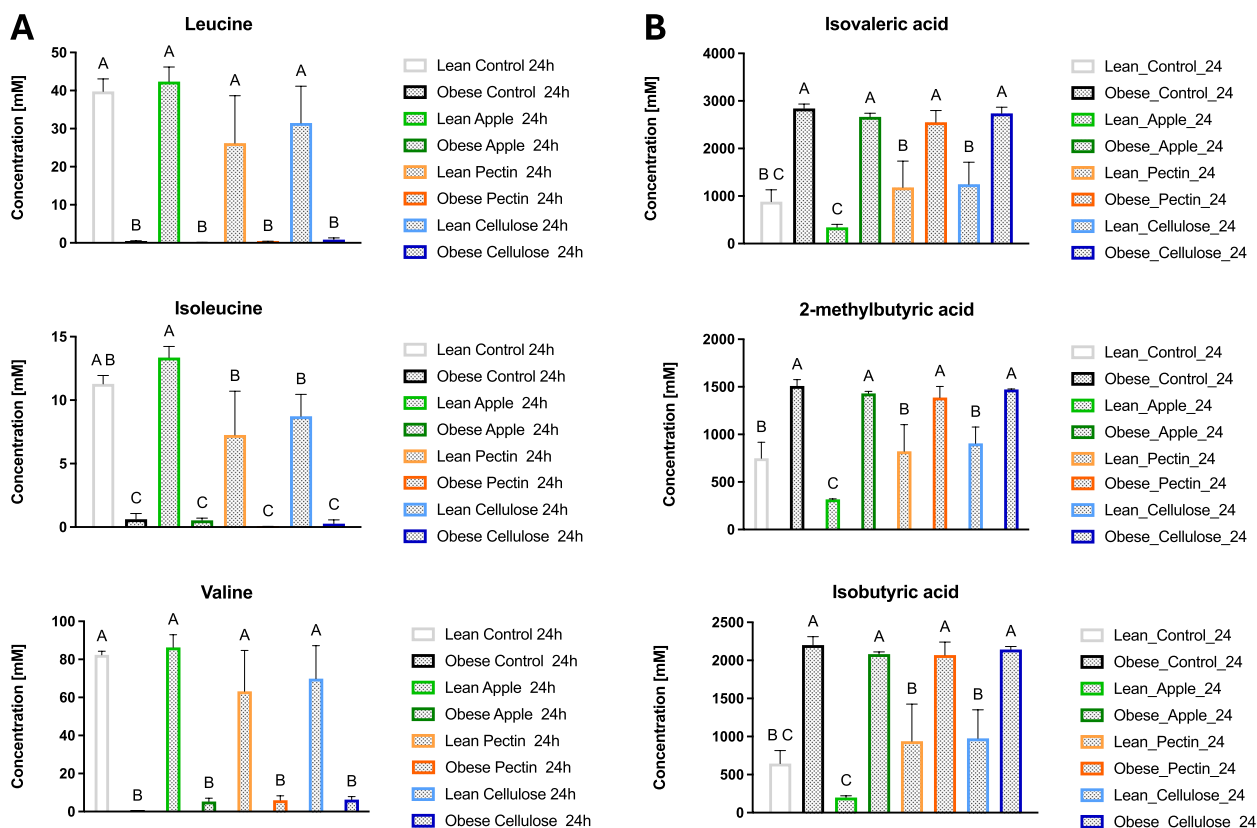


**Fig. 2** **A** Concentrations of BCAAs in lean and obese microbial communities after being exposed to different feeding conditions ( $t = 24$  h): this figure provides a graphical representation comparing the concentrations of BCAAs—leucine, isoleucine, and valine—in both lean and obese microbial communities after the administration of specific feeding conditions. Each bar in the graph represents the average concentration observed for a particular group and condition, with error bars depicting the standard deviation to illustrate the variability within each group. To identify statistical significance among the groups and conditions, the analysis involved multiple  $t$ -tests with Tukey correction for multiple comparisons. The results are visually indicated by different letters above each bar. Bars that share the same letter do not differ significantly from each other at a  $p$ -value  $\leq 0.05$ , suggesting that the feeding conditions had comparable effects on the concentrations of BCAAs in these groups. Conversely, bars adorned with different letters signify that the treatment groups exhibited statistically significant differences in BCAA concentrations, emphasizing the distinct impact of the feeding conditions. **B** Concentrations of BCFAs in lean and obese microbial communities after being exposed to different feeding conditions ( $t = 24$  h): this figure provides a graphical representation comparing the concentrations of BCFAs - isovaleric acid, 2-methylbutyric acid, and isobutyric acid - in both lean and obese microbial communities after the administration of specific dietary fibers. Similar to the BCAA graph, each bar represents the average concentration for a particular group and condition, with error bars showing the standard deviation. Statistical significance was assessed using multiple  $t$ -tests with Tukey correction, and different letters above each bar indicate significant differences ( $p$ -value  $\leq 0.05$ ). Data are representative of three independent fermentation experiments ( $n = 3$ ) using pooled fecal inoculum from either lean or obese groups

between the two types of microbial communities. The full dataset of the concentration before and after treatments and Tukey’s multiple comparisons for BA and HA are presented in Supplementary Data S8 and S9.

**Dietary fibers exert shifts in species and metabolites in both lean and obese microbial communities**

After exposing lean and obese microbial communities to different feeding conditions, we observed significant variations in microbial species and metabolic profiles. To further understand which bacterial species might be enriched by certain dietary fibers, we selected species of bacteria enriched using Microbiome Multivariable

Association with Linear Models (*MaAsLin2*) and Vulcano plots (Fig. 4). Our analysis highlighted considerable changes in the microbial communities upon administration of our feeding conditions in comparison to the control (Fig. 4). For the apple feeding condition, Fig. 4A, in the obese microbial community, *Klebsiella pneumoniae* ( $\text{Log}_2\text{FC} = 22$ ,  $\text{FDR} \leq 0.0001$ ), *Akkermansia muciniphila* ( $\text{Log}_2\text{FC} = 7.22$ ,  $\text{FDR} \leq 0.0001$ ), and *Bifidobacterium longum* ( $\text{Log}_2\text{FC} = 8.9$  ;  $\text{FDR} \leq 0.0001$ ) were highly responsive to apple. Conversely, *Bacteroides thetaiotaomicron* showed a significant decrease ( $\text{Log}_2\text{FC} = -11.3$ ,  $\text{FDR} \leq 0.0001$ ), suggesting a selective inhibitory effect. Additionally, *Acidaminococcus*

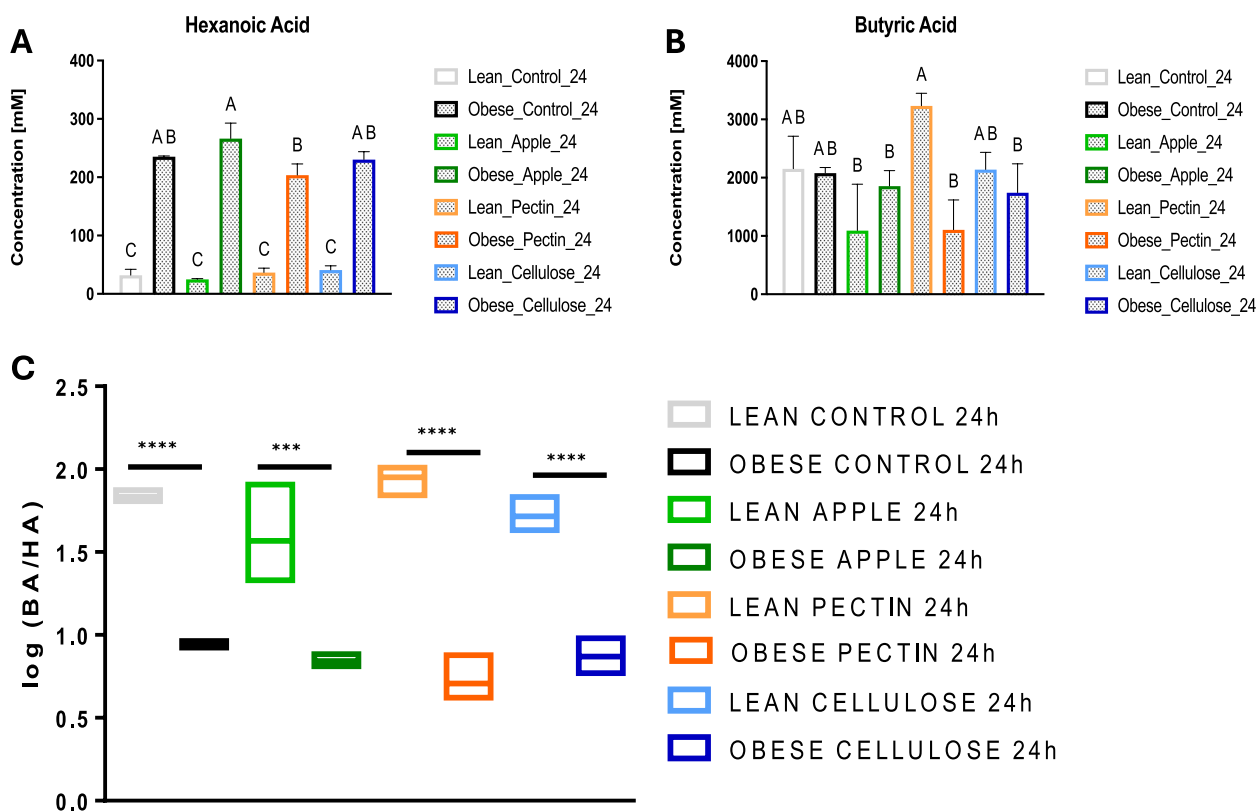


**Fig. 3** **A** Hexanoic acid (HA) concentrations across feeding conditions: This figure compares the effects of various feeding conditions on the hexanoic acid concentrations for lean and obese microbial communities. Each bar represents the average outcome observed under a specific feeding condition, with error bars depicting the standard deviation to convey the variability within each treatment group. To determine statistical significance among the treatments, multiple *t*-tests with Tukey correction for multiple comparisons were performed. Different letters above the bars indicate groups that are significantly different from each other at a *p*-value  $p \leq 0.05$ . Bars that share the same letter are not significantly different, suggesting comparable effects of those feeding conditions on the measured outcomes. Conversely, bars with different letters above them signify treatment groups with statistically significant differences in outcomes, thereby highlighting the distinct impacts of those feeding conditions on hexanoic acid concentrations. **B** Butyric acid (BA) concentrations across feeding conditions: This figure compares the effects of various feeding conditions on the butyric acid concentrations for lean and obese microbial communities with the same statistical significance markers and interpretation as described in Fig. 3A. **C** Log (BA/HA) ratio differences between lean and obese microbial communities and feeding conditions: This figure displays the effects of feeding conditions and microbial communities on the log (BA/HA) ratio. Significance levels are denoted by asterisks above the horizontal lines connecting relevant bars, with the following conventions: a single asterisk (\*) for  $p \leq 0.05$ , two asterisks (\*\*) for  $p \leq 0.01$ , three asterisks (\*\*\*) for  $p \leq 0.001$ , and four asterisks (\*\*\*\*) for  $p \leq 0.0001$ , indicating increasingly significant differences between the treatment effects. Data are representative of three independent fermentation experiments ( $n = 3$ ) using pooled fecal inoculum from either lean or obese groups

*intestini* also demonstrated a considerable decrease ( $\text{Log}_2\text{FC} = -8.83$ ;  $\text{FDR} \leq 0.0001$ ). When the obese microbial community was exposed to apple pectin, *Bacteroides thetaiotaomicron* and *Acidaminococcus intestini* showed marked reductions in abundance, with  $\text{log}_2$  fold changes ( $\text{Log}_2\text{FC}$ ) of  $-7.57$  and  $-8.15$ , respectively ( $\text{FDR} \leq 0.001$ ). In contrast, species such as *Megasphaera* sp. MJR8396C demonstrated a substantial increase ( $\text{Log}_2\text{FC} = 12.4$ ,  $\text{FDR} \leq 0.001$ ). Noteworthy increases were also found in *Slackia isoflavoniconvertens* ( $\text{Log}_2\text{FC} = 2.03$ ;  $\text{FDR} \leq 0.01$ ) in the apple pectin group. Upon cellulose feeding condition, *Bacteroides uniformis* exhibited the largest decrease

in abundance ( $\text{Log}_2\text{FC} = -4.36$ ,  $\text{FDR} \leq 0.01$ ), with *Parabacteroides distasonis* experiencing a significant increase ( $\text{Log}_2\text{FC} = 4.4$ ,  $\text{FDR} \leq 0.01$ ). In the lean microbial community, Fig. 4B, when exposed to the apple feeding condition, a significant reduction in the abundance of *Flavonifractor plautii* ( $\text{Log}_2\text{FC} = -6.2$ ,  $\text{FDR} \leq 0.0001$ ) and *Faecalibacterium prausnitzii* ( $\text{Log}_2\text{FC} = -5.52$ ,  $\text{FDR} \leq 0.0001$ ) suggested a strong impact of this feeding condition on this species. Conversely, *Bifidobacterium longum* demonstrated a substantial increase ( $\text{Log}_2\text{FC} = 6.85$ ,  $\text{FDR} \leq 0.0001$ ), indicating a positive response to the apple feeding condition in both lean and obese. The species

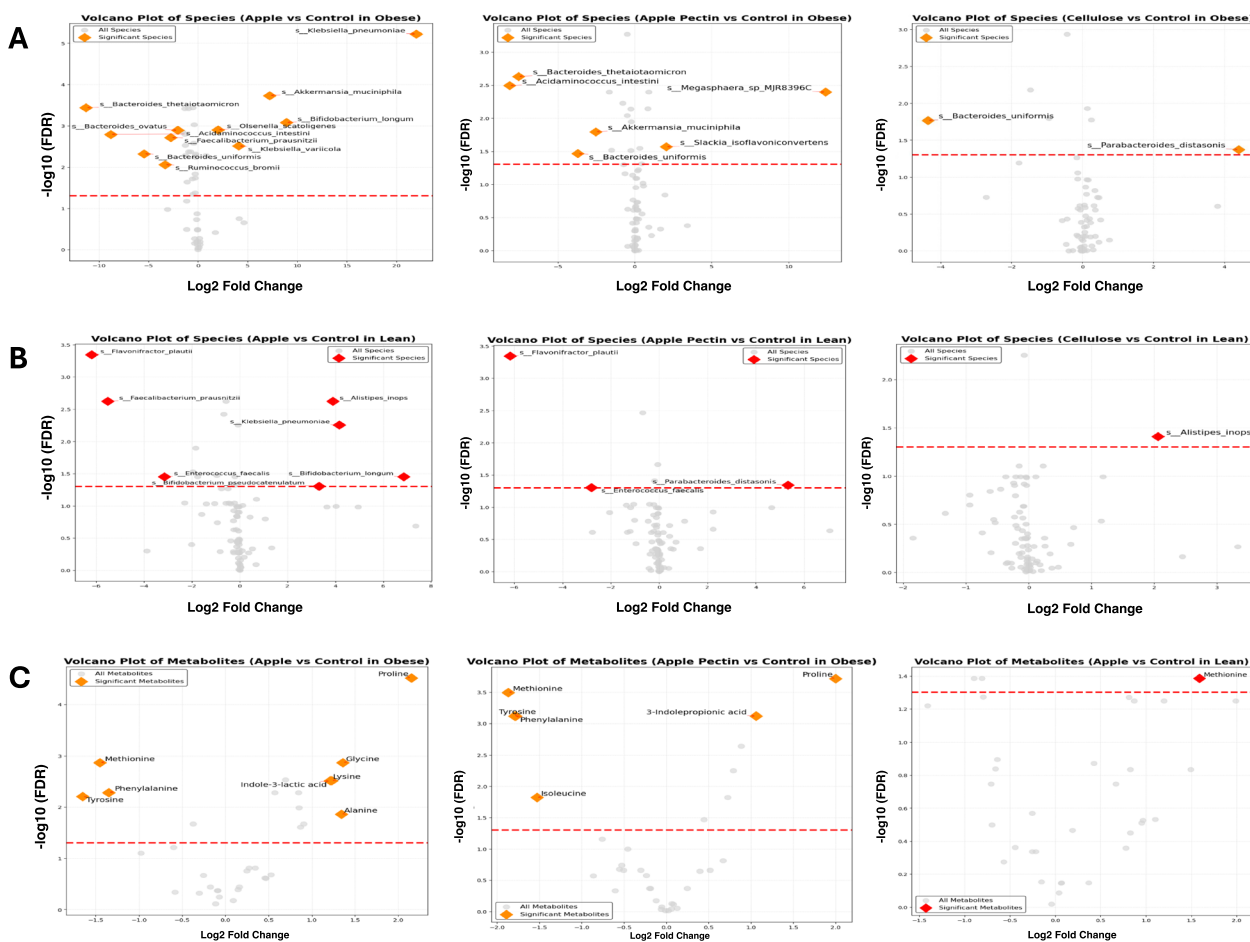


**Fig. 4** Comparison between enriched metabolites and species in obese and lean microbial communities after dietary fiber supplementation compared to the control. The conditions tested against the control included apple as a complex dietary matrix, apple pectin and cellulose as dietary fibers, following all the INFOGEST *in vitro* digestion. Only species and metabolites with  $FDR \leq 0.05$  and  $|Log_2FC| \geq 1$  were considered significant. The results highlight the significant metabolic changes induced by dietary fiber supplementation. Data are representative of three independent fermentation experiments ( $n = 3$ ) using pooled fecal inoculum from either lean or obese groups. **A** This panel shows volcano plots for enriched species in the obese microbial community. **B** Volcano plots for enriched species in the lean microbial community. **C** Volcano plots for enriched metabolites in lean or obese microbial communities

*Alistipes inops* showed a notable increase in abundance ( $Log_2FC = 3.9$ ,  $FDR \leq 0.0001$ ), while a decrease in *Alistipes putredinis* ( $Log_2FC = -1.77$ ,  $FDR \leq 0.0001$ ) was noticed. *Klebsiella pneumoniae* was again a species that significantly proliferated with apple supplementation ( $Log_2FC = 4.17$ ,  $FDR \leq 0.0001$ ), while *Enterococcus faecalis* was substantially reduced ( $Log_2FC = -3.15$ ,  $FDR \leq 0.00244$ ). In the apple pectin, a profound decrease in *Flavonifractor plautii* ( $Log_2FC = -6.18$ ,  $FDR \leq 0.01$ ) and *Enterococcus faecalis* ( $Log_2FC = -2.81$ ,  $FDR \leq 0.01$ ) was observed, whereas *Parabacteroides distasonis* showed a significant increase ( $Log_2FC = 5.33$ ,  $FDR \leq 0.001$ ). The cellulose feeding condition only increased *Alistipes inops* ( $Log_2FC = 2.06$ ,  $FDR \leq 0.01$ ) in the lean microbial community. These modifications underscore the specific

impact of dietary fibers on microbial composition. The detailed  $log_2$  fold changes, standard errors,  $p$ -values, and false discovery rates (FDR) for all analyzed microbial species are provided in Supplementary Data S10. To assess the metabolic impact of the different feeding conditions on both lean and obese microbial communities, the metabolomics results were analyzed using Linear Models for Microarray Data (LIMMA), a statistical method used to identify differentially expressed genes or metabolites, and Volcano plots (Fig. 4). A core capability of LIMMA is the use of linear models to assess differential expression in the context of multi-factor designed experiments. When we exposed the obese microbial community to the apple feeding condition (Fig. 4C), proline exhibited the greatest increase in concentration ( $Log_2FC = 2.15$ ,

FDR  $\leq$  0.00001), indicating a solid upregulation. Alanine ( $\text{Log}_2\text{FC} = 1.34$ , FDR  $\leq$  0.01), arginine ( $\text{Log}_2\text{FC} = 0.844$ , FDR  $\leq$  0.01), and glycine ( $\text{Log}_2\text{FC} = 1.36$ , FDR  $\leq$  0.001) significantly increased, whereas phenylalanine significantly decreased ( $\text{Log}_2\text{FC} = -1.35$ , FDR  $\leq$  0.01). In this frame, methionine and tyrosine showed marked decreases ( $\text{Log}_2\text{FC} = -1.45$  and  $-1.65$ , FDR  $\leq$  0.0001, respectively). Metabolites like IPA and ILA increased notably ( $\text{Log}_2\text{FC} = 0.696$  and  $1.21$ , respectively; FDR  $\leq$  0.001). SCFAs, such as propionic acid, showed a moderate increase ( $\text{Log}_2\text{FC} = 0.569$ , FDR  $\leq$  0.01). By exposing the obese microbial community to apple pectin (Fig. 4C), we observed that proline levels increased substantially ( $\text{Log}_2\text{FC} = 2$ , FDR  $\leq$  0.00001), indicating a pronounced response to the intervention compared to the control. Methionine, tyrosine, and phenylalanine levels decreased ( $\text{Log}_2\text{FC}$ s of  $-1.87$ ,  $-1.78$ , and  $-1.79$ , respectively, compared to the control; FDR  $\leq$  0.001 for all), suggesting a reduction in these amino acids compared to the control. Metabolites associated with gut microbial metabolism, such as IPA ( $\text{Log}_2\text{FC} = 1.06$ , FDR  $\leq$  0.001) and IAA ( $\text{Log}_2\text{FC} = 0.793$ , FDR  $\leq$  0.01) significantly increased. Among other amino acids, aspartic acid levels rose ( $\text{Log}_2\text{FC} = 0.668$ , FDR  $\leq$  0.05), whereas glutamine and tryptophan decreased ( $\text{Log}_2\text{FC}$ s of  $-0.759$  and  $-0.456$ , respectively; FDR  $\leq$  0.05). SCFAs presented mixed responses. For example, acetic acid ( $\text{Log}_2\text{FC} = 0.725$ , FDR  $\leq$  0.01) and propionic acid ( $\text{Log}_2\text{FC} = 0.445$ , FDR  $\leq$  0.01) increased, while butyric acid decreased ( $\text{Log}_2\text{FC} = -0.553$ , FDR  $\leq$  0.1). In comparison, for the lean microbial community, only the supplementation of apple had a significant effect on methionine ( $\text{Log}_2\text{FC} = 1.59$ , FDR  $\leq$  0.05). These alterations indicate how our feeding conditions exerted a varied impact on metabolite concentrations, mainly in the obese microbial community, reflecting the complex interplay between dietary fibers and the baseline microbial community. Metabolomics data indicated that apple and apple pectin supplementation had a stronger impact on the obese microbial community. The detailed  $\log_2$  fold changes, standard errors,  $p$ -values, and FDR) for all analyzed metabolites are provided in Supplementary Data S11.

#### Inter-omic data integration with procrustes and DIABLO

To evaluate the inter-omic concordance between our metagenomics and metabolomics datasets, we initially generated two-dimensional principal component plots (PC1 and PC2) from molecular function (KOs) and metabolomics data. Following this, we employed Procrustes analysis to assess the correlation between these datasets. Procrustes analysis aligns and resizes principal component plots, enabling the evaluation of non-random similarities between two independent measures. This

analysis indicated a high level of similarity ( $P = 0.001$ ) for both lean and obese microbiome and metabolome datasets, as demonstrated in Supplementary Figure S3. After establishing inter-omic concordance, we applied DIABLO, a supervised multivariate method that utilizes a multi-block partial least squares-discriminant analysis (PLS-DA) approach. This method discriminates samples based on class information and identifies variables contributing to group separations. DIABLO was instrumental in differentiating the studied conditions, namely apple, apple pectin, cellulose, and control, based on loading scores. We further investigated the relationship between features selected by DIABLO across data types. We visualized these features (KOs and metabolites) as shown in Fig. 5 for the obese microbial community and Supplementary Figure S4 for the lean microbial community. DIABLO PC1 (Fig. 5A and B) and PC2 (Fig. 5C and D) were highly discriminative for apple and apple pectin conditions, while PC3 (Fig. 5E and F) discriminated the cellulose and control. For the apple treatment, DIABLO Component 1 was highly discriminative, identifying a minimal set of features across data types that effectively separated the apple feeding condition from the other treatments (Fig. 5A). The correlation between KO and metabolome data for Component 1 highlighted key features associated with the apple treatment (Fig. 5B). Specifically, key KOs such as *L-arabinose isomerase* (K01804), involved in the isomerization of L-arabinose to L-ribulose, and *isoamylase* (K01214), which hydrolyzes alpha-1,6-glucosidic linkages in glycogen and related polysaccharides, were notable for their roles in metabolizing sugars such as xylose and sucrose. Additionally, *formate dehydrogenase-N, gamma subunit* (K08350), and *DNA sulfur modification protein DndD* (K19171) also contributed to the metabolic processes specific to the apple feeding condition. For the apple pectin treatment, DIABLO Component 2 identified features that distinguished apple pectin from the other treatments (Fig. 5C). The correlation data underscored apple pectin-relevant features and their associations (Fig. 5D). Important KOs such as *as acyl-CoA dehydrogenase* (K06446), involved in tryptophan metabolism, reflect the significant impact of apple pectin on microbial metabolic pathways connected to indoles. Other notable KOs for apple pectin included *2-aminobenzoylacetyl-CoA thioesterase* (K20257), an enzyme involved in the breakdown of aromatic compounds, and *glucoselysine-6-phosphate deglycase* (K19504), which plays a role in the detoxification of glycosylated proteins, thus might be indicating a metabolic adjustment in response to apple pectin. DIABLO Component 3 focused on distinguishing cellulose and control fermentation treatments from the other conditions (Fig. 5E). The correlation analysis illustrated the integrated features across

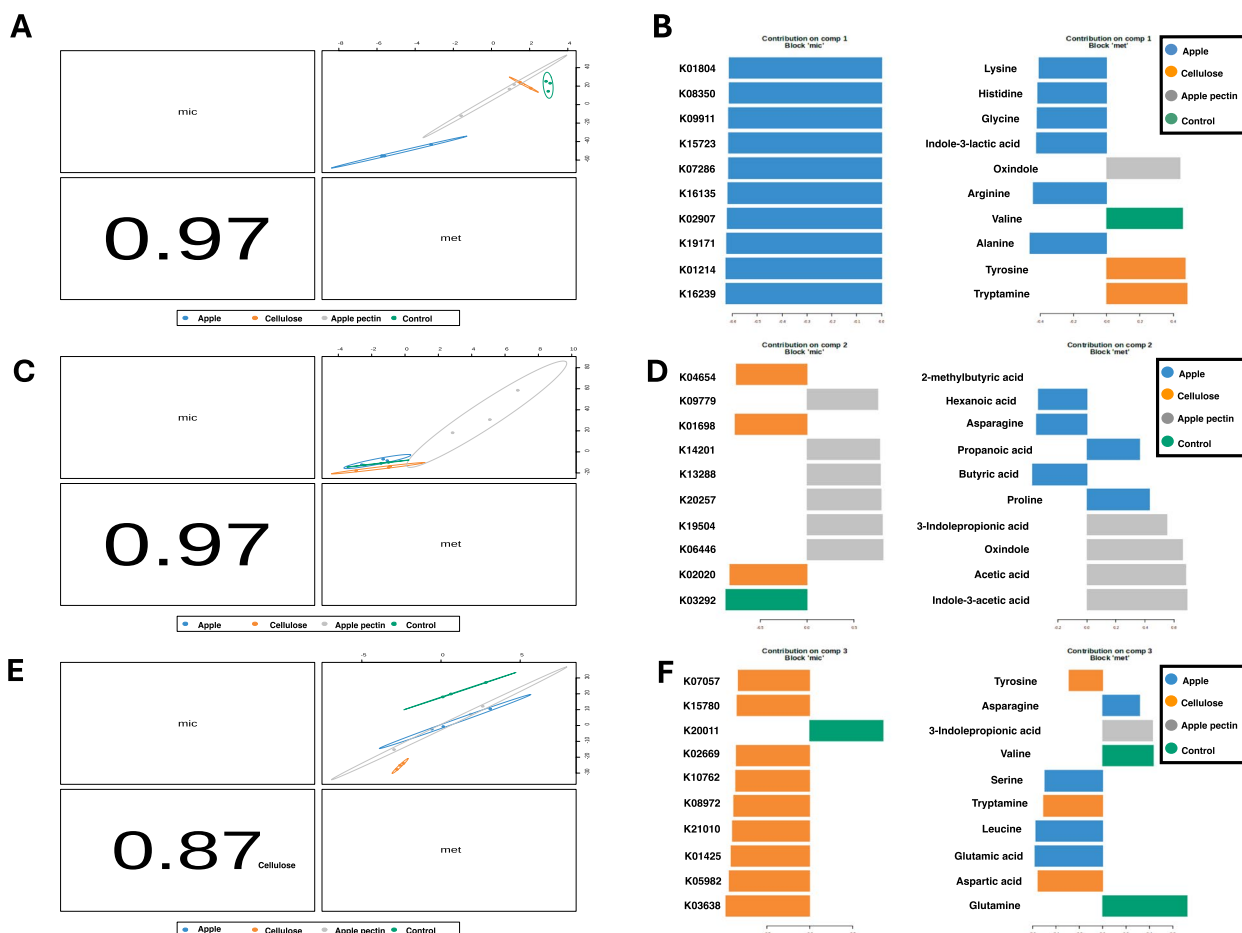


**Fig. 5** Data integration analysis for biomarker discovery using latent variable approaches (DIABLO) uncovered biologically relevant features by integrating information across microbiome potential functions (KO) and metabolome datasets to identify discriminative features between feeding conditions and the obese microbial community. **A** DIABLO Component 1: Dimensionality reduction performed to select a minimal set of features across data types that could discriminate between feeding conditions, specifically separating the apple feeding condition from the other treatments. **B** Correlation of KO and metabolome data for Component 1, showing the association between these data types and highlighting the key features of apple treatment. **C** DIABLO Component 2: Features selected to discriminate apple pectin from the other feeding conditions. **D** Correlation of KO and metabolome data for DIABLO Component 2, indicating the apple pectin’s relevant features and their associations. **E** DIABLO Component 3: Features selected to discriminate cellulose and control fermentation from the other treatments. **F** Correlation of KO and metabolome data for DIABLO Component 3, illustrating the integrated analysis across data types. Data are representative of three independent fermentation experiments ( $n = 3$ ) using pooled fecal inoculum from either lean or obese groups

data types (Fig. 5F). Key KOs for cellulose feeding conditions included *glutaminase* (K01425), which catalyzes the hydrolysis of glutamine to glutamate, and *polysaccharide biosynthesis protein PeE* (K21010), involved in the biosynthesis of exopolysaccharides, essential for cellulose breakdown and utilization. Other relevant KOs for cellulose treatment were *molybdate transport system substrate-binding protein* (K02020), involved in molybdate transport, which is essential for various enzyme functions, and *N4-bis(aminopropyl)spermidine synthase* (K07057), which plays a role in polyamine biosynthesis important for cell growth and differentiation. This integrated analysis across KOs and metabolome data

provided a comprehensive understanding of the metabolic pathways and functions that differentiate these dietary treatments.

**Genome scale modelling of *Megasphaera* spp.**

After assessing the distinct effect of apple pectin on the obese microbial community and linking it with *Megasphaera* sp. MJR8396C, we tried to understand if its enrichment in apple pectin was possibly related to specific metabolic capabilities. We first investigated its primary metabolism using GutSMASH [45, 46]. From the genome mining, we noted the presence of two gene clusters, a nitrogenase-like complex (Rnf) with 83%

homology to the one present in *Clostridium sporogenes* [51] and the leucine reductive branch from *Clostridium difficile* with 50% similarity, as shown in Figure S5. Both findings pointed toward a clostridium-like metabolism capable of amino acid fermentation. To better study the metabolic capabilities of this species, we reconstructed its metabolic genome-scale model (GSM) using CarveMe, and we computed its growth using BacArena in a simulated gut medium over 24 h batch conditions. This modeling approach enabled us to explore the metabolic pathways and potential interactions with other gut microbes. Given that *Megasphaera* growth was recently discovered to rely on metabolites generated by *Bifidobacteria*, and in our study, *Bifidobacterium adolescentis* was the most abundant species present after the in vitro fermentation of apple pectin, as shown in Fig. 1E, we also simulated a co-culture of *Megasphaera* sp. MJR8396C with *Bifidobacterium adolescentis* to examine possible cross-feeding interactions in silico. Intriguingly, the simulation demonstrated how the two species exert two different cross-feeding mechanisms, as shown in Fig. 6 when they are associated. As shown in Fig. 6A, *Bifidobacterium adolescentis* is capable of producing mainly

acetate and lactate from the simulated gut medium in co-culture, while *Megasphaera* sp. MJR8396C produces butyrate, fumarate, and ammonia. Instead, Fig. 6B shows how the primary metabolites consumed by both *Bifidobacterium adolescentis* and *Megasphaera* sp. MJR8396C over 24 h of batch fermentation are mainly glutamate and sucrose with additional requirements for essential AAs. From the BacArena simulation, in Fig. 6C and D, two main cross-feeding mechanisms are shown when the two species are grown together. For the first mechanism, as shown in 6C, *Megasphaera* benefits from fumarate produced by *Bifidobacterium*, a metabolite critical for its energy metabolism. In contrast, *Bifidobacterium* may benefit from hydrogen sulfide and ammonia released by *Megasphaera*. In the second mechanism (Fig. 6D), the exchange of acetate and lactate by *Bifidobacterium* and the provision of formate and ammonia by *Megasphaera* suggest another reciprocal relationship that would better explain the metabolomics results. *Megasphaera* may benefit from the availability of acetate and lactate, together with the presence of amino acids in the medium, for energy generation. In contrast, *Bifidobacterium* could benefit from formate and ammonia for the same purpose.

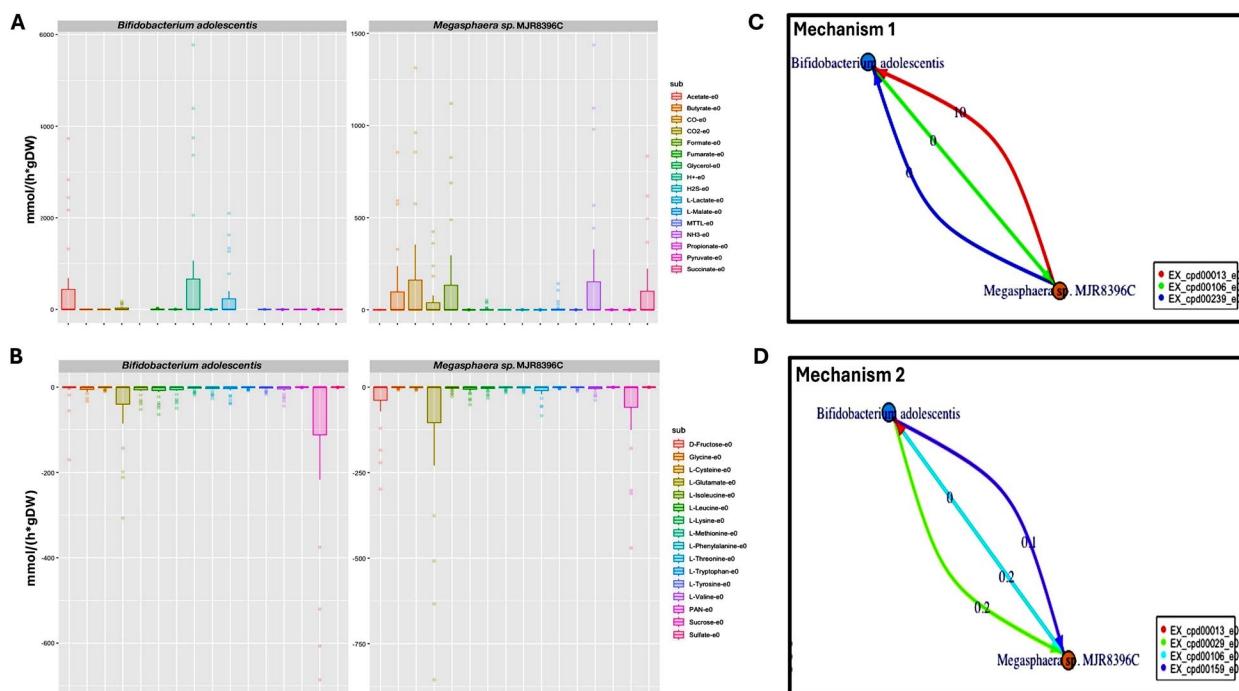


**Fig. 6** Metabolites secreted and consumed by *Bifidobacterium adolescentis* and *Megasphaera* sp. MJR8396C during an in silico simulation on their growth over 24 h batch fermentation, and the cross-feeding mechanisms between the two species simulated using BacArena. **A** Metabolites secreted by *Bifidobacterium adolescentis* and *Megasphaera* sp. MJR8396C over 24 h of batch fermentation. **B** Metabolites consumed by *Bifidobacterium adolescentis* and *Megasphaera* sp. MJR8396C over 24 h of batch fermentation. **C** Cross-feeding mechanism 1, where *Megasphaera* receives cpd00106 (Fumarate) and *Bifidobacterium* receives cpd00239 (Hydrogen Sulfide) and cpd00013 (Ammonia). **D** Cross-feeding mechanism 2, where *Megasphaera* receives cpd00029 (Acetate) and cpd00159 (Lactate), and *Bifidobacterium* receives cpd00106 (Fumarate) and cpd00013 (Ammonia)

This co-culture modeling approach provides valuable insights into the metabolic interactions and dependencies between *Megasphaera sp. MJR8396C* and *Bifidobacterium adolescentis*, highlighting the significance of cross-feeding mechanisms in their synergistic relationship within the obese microbial community. The sum exchanges for each species and metabolite over all the 400 grid cells are provided in Supplementary Data S13.

## Discussion

In this *in vitro* work, we combined metagenomics, targeted metabolomics, and genome-scale metabolic modeling to investigate the complex interactions between dietary fibers (apple pectin, cellulose, and an apple as a food model) and lean and obese microbial communities. By pooling fecal samples from clinically characterized lean and obese individuals, we aimed to create representative microbial communities for each group, as previously reported [26]. While pooling helped capture broader microbial characteristics, we recognize that this approach also introduces limitations, particularly concerning the ability to generalize our findings to the broader population of lean and obese individuals. The obese microbial community had a consistently higher abundance of *Ruminococcus bromii* compared to the lean group, which is in line with previous investigations that found higher abundances of *R. bromii* in stools of obese subjects [8, 52]. Moreover, the obese microbial community highlighted a lower abundance of *Faecalibacterium prausnitzii*, which is a trait commonly associated with intestinal dysbiosis [53–55]. Apart from differences at the species level, we verified an elevated *Firmicutes:Bacteroides* ratio in the obese microbial community. This ratio indicates the relative abundance of two major bacterial phyla in the human gut microbiota and the characteristic of intestinal disbalance in obesity [56–58]. One important difference when comparing obese and lean microbial communities was the variation in metabolic signatures. The obese microbial community showed enhanced BCAA catabolism and BCFA production. In the context of obesity, research conducted on human fecal samples has revealed how the increased BCFA concentration is widespread in obese subjects, even though only a few direct relationships to the gut microbiota have been pointed out [52, 59, 60]. Concerning BCAAs, only a few studies have described how BCAAs can be metabolized by the gut microbiome [61–63]. Pedersen and co-authors demonstrated that a gut microbiome with an increased capacity for BCAA biosynthesis and fewer bacterial transporters for these amino acids is associated with higher plasma BCAA levels [63]. Importantly, this potential for increased BCAA production and

reduced bacterial uptake is linked to insulin resistance [63]. Similarly, Ridaura et al. found that mice exhibited elevated circulating BCAA levels after receiving stool transplants from individuals with insulin resistance, indicating a microbial influence on BCAA metabolism [64]. Microorganisms capable of fermenting BCAAs have been identified and linked to diets rich in high-protein sources [65–67]. For example, colonic fermentation of amino acids was recently explored using proteolytic clostridia found in the human gut [51]. Liu et al. employed metabolomics to show that *C. sporogenes* can metabolize amino acids, including BCFAs, through the Stickland reaction, producing metabolites that may be absorbed and circulate in the bloodstream [51, 68]. Furthermore, *C. sporogenes* may convert BCAAs (valine, isoleucine, and leucine) to BCFAs (isobutyric acid, 2-methylbutyric acid, and isovaleric acid) [51, 68]. Collectively, these observations indicate that the gut microbiota of obese and lean subjects play a crucial role in altering BCAA and BCFA levels at the host level. We suspect the metabolic traits of the obese microbial community observed in our study may be enriched with species that transform BCAAs into BCFAs through a *Clostridium*-like metabolism. This insight opens exciting avenues for exploring how specific gut microbiota can influence metabolic health and potentially pave the way for innovative interventions in combating obesity. When comparing SCFAs and medium-chain fatty acids (MCFAs), we discovered that the BA/HA ratio varied noticeably between lean and obese microbial communities. HA has not been extensively studied in relation to obesity and gut microbiota, but a few studies have explored its potential role in describing changes in gut microbiota. Rios et al. assessed the fecal concentration of SCFAs and MCFAs in 232 healthy individuals with BMI ranging from 19 to 54 [69]. The study showed how the molar proportions of HA compared to the other MCFAs increased throughout BMI [69]. In another similar investigation, the BA/HA ratio has been impaired in peripheral blood serum samples from multiple sclerosis (MS) patients [70]. Interestingly, the MS patients had lower serum concentrations of BA and higher concentrations of HA, together with an altered gut microbiota. This included changes in the abundance of butyrate producers, changes in barrier permeability (higher plasma concentrations of lipopolysaccharide), intestinal fatty acid-binding protein, and inflammation [70]. Although the pathway leading to HA synthesis is not well studied in the context of the human gut microbiota and obesity, recent research described the ability of a newly isolated *Ruminococcaceae* strain affiliated with *Clostridium cluster IV* to produce HA from lactate utilization [71].



Furthermore, Scarborough et al. demonstrated that anaerobic microbial communities can produce hexanoic acid from complex carbohydrates using reverse  $\beta$  oxidation [72]. Our findings suggest that the variations observed in the BA/HA ratio, attributed solely to bacterial activity in our in vitro system, may indicate a microbial contribution to the rise in HA observed in obesity. However, it is important to emphasize that these findings, based on pooled samples and in vitro conditions, may not fully capture the complexity of individual microbial responses in vivo. This shift results in a markedly altered metabolism compared to the lean group. Notably, the mechanism described by Scarborough et al. highlights that HA production (C6) yields a two-fold increase in ATP production compared to BA production (C4) when lactate is the sole substrate [72]. This suggests a significant role for lactate in HA synthesis within the obese gut microbiota. In general, MCFAs showed more distinctive trends than SCFA (acetate, propionate, and butyrate), and our study suggests MCFAs might be indicators of altered microbial composition and metabolism in obese. After defining the key functional features distinguishing obese from lean microbial communities, our findings revealed that apple dietary fibers profoundly impact these microbial communities, with apple and apple pectin feeding conditions showing the most significant effects. The impact of apple pectin on the gut microbiota, both at the taxonomic and functional levels, was significantly influenced by whether the starting microbial population came from lean or obese individuals. In the obese microbial community, apple pectin significantly decreased the abundance of *Acidaminococcus intestini* and *Bacteroidetes thetaiotaomicron* while strongly increasing the abundance of *Megasphaera* MJR8396C. The same treatment in lean individuals decreased the abundance of *Flavonifractor plautii* and significantly increased the abundance of *Parabacteroides distasonis*. These findings suggest that the impact of dietary fibers is particularly dependent on the initial microbial composition of the gut [8]. Our study revealed a striking observation since apple and apple pectin induced significant changes in both microbial species and metabolites in the obese microbial community. In contrast, in the lean microbial community, these feeding conditions primarily altered microbial species with minimal impact on metabolite profiles. This highlights the significant potential of dietary fibers to influence intestinal microenvironments, especially in the context of obesity. This might point towards a stronger effect of dietary fiber on the obese microbial community compared to the lean one. However, we must acknowledge that these observations are based on the pooled sample

design, and the effects of dietary fibers might differ in individual microbiomes. The apple feeding condition, apart from decreasing the relative abundance of *Acidaminococcus intestini* and *Bacteroidetes thetaiotaomicron*, increased the relative abundance of *Akkermansia muciniphila*, which was significant in the obese microbial community. In general, several studies showed a negative association between the abundance of *Akkermansia muciniphila* and obesity, which might indicate a positive modulatory effect of apple pectin, and potentially other pectins in obesity [73–76]. In addition to modulations specific to either the lean or obese microbial communities, the apple feeding condition consistently influenced certain species, such as *Klebsiella pneumoniae*. This species, frequently regarded as an opportunistic pathogen, raises questions concerning the precise mechanism by which the apple matrix can regulate the abundance of opportunistic bacteria within the gut ecosystem. To answer this question, among the main traits chosen by DIABLO to discriminate apple treatment in obese, we discovered an enrichment of *bsdC* (K016239), a hydroxybenzoate decarboxylase. This enzyme belongs to the lyase family, specifically carboxy-lyases, which break carbon-carbon bonds. Interestingly, it is responsible for the non-oxidative decarboxylation of phenolic acids, such as hydroxybenzoic, protocatechuic, and gallic acid, which are present in the apple matrix [77]. Phenolics are commonly associated with cell wall components, including cellulose, hemicellulose, arabinoxylans, structural proteins, and pectin through ester, ether, and C-C linkages [78]. This enzyme is found in the genome of *Klebsiella pneumoniae* [77], but is also found in other opportunistic pathogens [79]. We believe that the consistent bloom of a specific opportunistic bacteria, such as *Klebsiella pneumoniae*, observed after apple supplementation may be connected to the activation of pathways providing resistance to polyphenolic compounds. The hydroxybenzoate decarboxylase may provide a competitive advantage to *Klebsiella pneumoniae* in assimilating the phenolics released from the apple condition [80]. In contrast, with the enrichment of *Klebsiella*, the apple feeding condition consistently modulated the abundance of *Bifidobacterium longum*. This species seems to have a negative correlation with obesity and has recently shown anti-obesity benefits in obese mice fed a high-fat diet by lowering body weight, reducing fat depot buildup, and improving glucose tolerance, highlighting again a possible positive effect exerted by the dietary fiber ability to re-shape the obese microbial community [81]. In addition to modulating species, our study found that both apple and apple pectin in the obese microbial community led to a significant

decrease in phenylalanine, tyrosine, and methionine. Concurrently, there was an increase in glycine, proline, and alanine. Interestingly, apple and apple pectin feeding conditions significantly increased the production of IPA, ILA, and IAA in the obese microbial community. According to DIABLO findings, the apple pectin feeding condition was correlated to an enrichment in the Acyl-CoA dehydrogenase enzyme. This finding aligns with the increased presence of IPA, as acyl-CoA dehydrogenase (K06446) is one of the final steps in the conversion of aromatic amino acids (AAs) into IPA by intestinal microorganisms [82]. Recent studies have also shown a tight connection between the consumption of dietary fibers and the modulation of indole metabolites [21, 82]. The effects of pectin, inulin and their combination on the production of microbiota-derived indoles and SCFAs were investigated in a fecal batch system inoculated with microbial communities isolated from the Simulator of Human Intestinal Microbial Ecosystem [21]. Consistent with our findings, Huang et al. reported that pectin supplementation significantly increased the production of other indolic compounds, including IAA and IA [21]. In this frame, Sinha et al. have recently demonstrated that the production of IPA and ILA was primarily influenced by dietary fiber's regulation using co-culture experiments and fecal samples [83]. This regulation is based on substrate availability rather than the quantity of tryptophan. In the gut environment, *Escherichia coli*, which produces indole, and *C. sporogenes*, which synthesizes ILA and IPA, compete for tryptophan. The fiber-degrading *Bacteroides thetaiotaomicron* alters this competition by supplying monosaccharides to *E. coli*, thereby reducing indole production through catabolite repression. This shift allows more tryptophan to be available for *C. sporogenes*, leading to increased production of ILA and IPA [83]. Our results affirm the role of apple fibers, particularly pectin, in modulating species capable of influencing the metabolism of aromatic AAs and enhancing the synthesis of indolic acids. Interestingly, while our experiment did not show significant changes in indole synthesis, it suggests a distinct mechanism possibly involving other microbial species compared to the study of Sinha et al., especially in the obesity context [24, 51, 83]. Aromatic AAs, along with IPA and ILA, have garnered significant attention for their association with gut barrier integrity, cognitive performance, and their potential preventive effects against disease [82, 84]. In the context of obesity, Arno-riaga-Rodríguez et al. identified a distinct microbiota profile linked to memory through pathways involving aromatic AAs and one-carbon metabolism. Importantly, these relationships were found to be influenced

by obesity [84]. The interplay between the intestinal microbiota, diet, and the brain is now recognized as a crucial factor in cognitive health [85]. Our study highlights that dietary modulation is a viable strategy to alter aromatic AA bacterial metabolism in the obese microbial community, potentially impacting the host at several levels, like the gut-brain axis [85]. In our investigation, the impact of apple pectin in obese microbial community was characterized by a notable co-enrichment of *Megasphaera* sp. MJR8396C and *Bifidobacterium adolescentis*, which we identified as capable of cross-feeding based on computational modeling. This approach builds on previous findings where *Megasphaera*, known for being a potential butyrate producer, exhibited increased growth and butyrate production when utilizing metabolites like lactate generated by *Bifidobacteria*. This supports the hypothesis of a mutualistic cross-feeding relationship between these microbial species [86, 87]. Although the role of *Megasphaera* spp. is still not clear in the context of the human gut microbiota and obesity, a few studies point towards its cooperative lifestyle with *Bifidobacteria* based on lactate exchange [86, 87]. Our in silico findings also showed that in the context of obesity, *Megasphaera* sp. MJR8396C has strong requirements for AAs and simple sugars. Therefore, besides lactate, which has been recently demonstrated, there may be other cross-feeding mechanisms between *Megasphaera* and *Bifidobacteria* [86, 87]. Furthermore, our investigation of *Megasphaera* revealed the presence of gene clusters homologous to those found in *C. sporogenes*, related to Stickland metabolism. These findings suggest a potential key role for *Megasphaera* sp. MJR8396C in competing with other species for aromatic AA metabolism, directly affecting ILA and IPA production. We acknowledge that confirming it will require tailored in vitro experiments once the isolation of this species becomes possible. Overall, our results emphasize how dietary components, such as apple fibers (apple pectin and apple as a food model), may profoundly reshape an obese microbial community, influencing both the microbial composition and the resultant metabolic profiles (e.g., amino acids, indolic acids), which may significantly impact the host [6]. The approach used in this study effectively characterized a baseline gut microbiota that accurately represented both obese and lean microbial communities at functional and taxonomical levels. This enabled us to investigate the baseline metabolic functionality and the impact of dietary fibers (cellulose, apple pectin, and apple) on the gut microbiota and their potential implications for the host. Firstly, the obese microbial community showed enhanced BCAA

catabolism and higher BCFA and HA production compared to the lean microbial community, demonstrating a baseline metabolism irrespective of the feeding conditions. High production of HA may impact the host's overall energy balance and influence energy homeostasis. Secondly, apple dietary fibers, particularly apple pectin, had a profound impact. In the obese microbial community, apple pectin significantly altered microbial species and metabolites, while in the lean community, it primarily affected microbial species. Apple pectin, but also apple, consistently modulated certain species, such as *Klebsiella pneumoniae*, an opportunistic pathogen, and *Bifidobacterium longum*, which is negatively correlated with obesity. The enrichment of specific bacterial enzymes suggests a mechanism by which dietary fibers modulate microbial composition and, in turn, gut-related metabolites, such as IPA and ILA. Our study identified a notable co-enrichment of *Megasphaera* sp. MJR8396C and *Bifidobacterium adolescentis* in the obese microbial community, suggesting mutualistic cross-feeding, particularly through lactate exchange. Gene clusters related to Stickland metabolism in *Megasphaera* indicate a competitive role in aromatic AA metabolism, impacting ILA and IPA production. This study provides valuable insights into how dietary fibers affect the gut microbiome in the context of obesity. However, there are some limitations to consider. First, our in vitro model, which uses pooled fecal samples, may not fully represent the complex gut environment of both obese and lean individuals. Additionally, demographic differences, particularly in age and body composition among participants, could influence microbiome and metabolic responses. While our findings indicate that the pooled inoculum reflects characteristics of the obese microbiome, future studies should consider a larger cohort considering sex and age to investigate their potential effects. This model may also overlook the influence of less abundant but significant microbial species that vary widely among different people. Finally, the responses to dietary fibers observed in this controlled environment may differ in vivo. In summary, while our study offers valuable insights into the interactions between dietary fibers and the gut microbiome in the context of obesity, the reliance on pooled fecal samples and in vitro conditions limits the extent to which these findings can be generalized. Future studies with larger sample sizes and individual-level analyses are needed to confirm these results and explore the potential for personalized dietary interventions to modulate the gut microbiome and improve metabolic health. Despite the limitations, our study demonstrates that dietary interventions can

strategically influence host health by altering microbial composition and biochemical pathways. These findings reinforce the critical role of food as a major determinant of gut microbiota, underscoring its impact on human health and disease. Our findings open new avenues for dietary interventions aimed at attenuating obesity and improving overall health using a personalized approach that may lead to more effective strategies for modulating gut microbiota and improving metabolic health.

### Supplementary Information

The online version contains supplementary material available at <https://doi.org/10.1186/s40168-024-01975-x>.

- Supplementary Material 1.
- Supplementary Material 2.
- Supplementary Material 3.
- Supplementary Material 4.

### Acknowledgements

Dr. Rubert would like to thank CIBIO - Department of Cellular, Computational, and Integrative Biology, University of Trento, Via Sommarive 9, Povo 38123, Italy, and the Interdisciplinary Research Structure of Biotechnology and Biomedicine, Department of Biochemistry and Molecular Biology, Universitat de Valencia, 46100 Burjassot, València, Spain, for their support and the resources provided during the different stages of this research. The authors would like to thank Dr. Mireia Valles-Colomer for advising on using bioBakery Workflows.

### Authors' contributions

AD performed the bioinformatics work (formal analysis, visualization, and data curation), methodology, investigation, conceptualization, writing—review and editing, and writing—original draft. W.S. Jr performed the GSMS, writing—review and editing. ST-F performed sample collection and statistics on clinical data, writing - review and editing. NSO performed sample collection and statistics on clinical data, writing—review and editing. JS performed the statistics on clinical data, writing—review and editing. JR performed supervision, resources, project administration, methodology, investigation, funding acquisition, formal analysis, data curation, conceptualization, writing—review and editing, and writing - original draft.

### Funding

Dr. Rubert acknowledges the support of the 'European Union's Horizon 2020 Research and Innovation programme' for the Marie Skłodowska-Curie grant agreement No 79441 and the Spanish Ministry of Science and Innovation for the Ramón y Cajal fellowship (RYC2018-024850-I) provided.

### Data availability

The metagenomics raw sequences are available at NCBI under the bioproject accession PRJNA1089942. Materials described in the manuscript, including all relevant raw data, will be freely available as Supplementary Figures (.pdf) and Data (.xlsx). The in silico experiments are publicly available at Zenodo repository 10.5281/zenodo.12749238. The genome-scale metabolic models for *Megasphaera* MJR8396C and *Bifidobacterium adolescentis* ATCC 15703F are deposited at Biomodels (MODEL2407160001, MODEL2407160002) and available for reviewers upon request. The models will be released to the public after publication to adhere to FAIR standards.

### Declarations

#### Ethics approval and consent to participate

The study has been approved by the ethical committee of the University of Trento with the protocol number 2018-026.

**Consent for publication**

All the authors gave written consent before publication of the work.

**Competing interests**

The authors declare that they have no competing interests.

**Author details**

<sup>1</sup>Food Quality and Design, Wageningen University & Research, Wageningen, The Netherlands. <sup>2</sup>Division of Human Nutrition & Health, Wageningen University & Research, Wageningen, The Netherlands. <sup>3</sup>Systems and Synthetic Biology, Wageningen University & Research, Wageningen, The Netherlands. <sup>4</sup>UNLOCK, Wageningen University & Research, Wageningen, The Netherlands. <sup>5</sup>Lluís Alcanyis Foundation-University of Valencia, University Clinic of Nutrition, Physical Activity and Physiotreatment, Valencia, Spain. <sup>6</sup>Food and Health Laboratory, Institute of Materials Science, University of Valencia, Valencia, Spain. <sup>7</sup>Department of Community Nursing, Preventive Medicine and Public Health and History of Science, University of Alicante, Alicante, Spain. <sup>8</sup>Joint Research Unit on Endocrinology, Nutrition and Clinical Dietetics, Health Research, Institute La Fe, University of Valencia, Valencia, Spain.

Received: 9 July 2024 Accepted: 12 November 2024

Published online: 30 November 2024

**References**

- Rooks MG, Garrett WS. Gut microbiota, metabolites and host immunity. *Nat Rev Immunol*. 2016;16(6):341–52.
- Wastyk HC, Fragiadakis GK, Perelman D, Dahan D, Merrill BD, Feiqiao BY, et al. Gut-microbiota-targeted diets modulate human immune status. *Cell*. 2021;184(16):4137–53.
- Eckburg PB, Bik EM, Bernstein CN, Purdom E, Dethlefsen L, Sargent M, et al. Diversity of the human intestinal microbial flora. *Science*. 2005;308(5728):1635–8.
- Roager HM, Christensen LH. Personal diet-microbiota interactions and weight loss. *Proc Nutr Soc*. 2022;81(3):243–54.
- David LA, Materna AC, Friedman J, Campos-Baptista MI, Blackburn MC, Perrotta A, et al. Host lifestyle affects human microbiota on daily time-scales. *Genome Biol*. 2014;15(7):1–15.
- David LA, Maurice CF, Carmody RN, Gootenberg DB, Button JE, Wolfe BE, et al. Diet rapidly and reproducibly alters the human gut microbiome. *Nature*. 2014;505(7484):559–63.
- Armet AM, Deehan EC, O'Sullivan AF, Mota JF, Field CJ, Prado CM, et al. Rethinking healthy eating in light of the gut microbiome. *Cell Host Microbe*. 2022;30(6):764–85.
- Walker AW, Ince J, Duncan SH, Webster LM, Holtrop G, Ze X, et al. Dominant and diet-responsive groups of bacteria within the human colonic microbiota. *ISME J*. 2011;5(2):220–30.
- Makki K, Deehan EC, Walter J, Bäckhed F. The impact of dietary fiber on gut microbiota in host health and disease. *Cell Host Microbe*. 2018;23(6):705–15.
- Ley RE, Bäckhed F, Turnbaugh P, Lozupone CA, Knight RD, Gordon JL. Obesity alters gut microbial ecology. *Proc Natl Acad Sci*. 2005;102(31):11070–5.
- Ley RE, Turnbaugh PJ, Klein S, Gordon JL. Human gut microbes associated with obesity. *Nature*. 2006;444(7122):1022–3.
- Palau-Rodríguez M, Tulipani S, Isabel Queipo-Ortuño M, Urpi-Sarda M, Tinahones FJ, Andres-Lacueva C. Metabolomic insights into the intricate gut microbial-host interaction in the development of obesity and type 2 diabetes. *Front Microbiol*. 2015;6:154996.
- Zhang B, Jiang M, Zhao J, Song Y, Du W, Shi J. The mechanism underlying the influence of indole-3-propionic acid: A relevance to metabolic disorders. *Front Endocrinol*. 2022;13:841703.
- Duncan SH, Lobleby G, Holtrop G, Ince J, Johnstone A, Louis P, et al. Human colonic microbiota associated with diet, obesity and weight loss. *Int J Obes*. 2008;32(11):1720–4.
- Turnbaugh PJ, Gordon JL. The core gut microbiome, energy balance and obesity. *J Physiol*. 2009;587(17):4153–8.
- Tremaroli V, Bäckhed F. Functional interactions between the gut microbiota and host metabolism. *Nature*. 2012;489(7415):242–9.
- Bradlow HL. Obesity and the gut microbiome: pathophysiological aspects. *Hormon Mol Biol Clin Investig*. 2014;17(1):53–61.
- Zhang LS, Davies SS. Microbial metabolism of dietary components to bioactive metabolites: opportunities for new therapeutic interventions. *Genome Med*. 2016;8:1–18.
- Koh A, De Vadder F, Kovatcheva-Datchary P, Bäckhed F. From dietary fiber to host physiology: short-chain fatty acids as key bacterial metabolites. *Cell*. 2016;165(6):1332–45.
- Huang Z, Boekhorst J, Fogliano V, Capuano E, Wells JM. Distinct effects of fiber and colon segment on microbiota-derived indoles and short-chain fatty acids. *Food Chem*. 2023;398:133801.
- Huang Z, Boekhorst J, Fogliano V, Capuano E, Wells JM. Impact of high-fiber or high-protein diet on the capacity of human gut microbiota to produce tryptophan catabolites. *J Agric Food Chem*. 2023;71(18):6956–66.
- Weitkunat K, Stuhlmann C, Postel A, Rumberger S, Fankhänel M, Woting A, et al. Short-chain fatty acids and inulin, but not guar gum, prevent diet-induced obesity and insulin resistance through differential mechanisms in mice. *Sci Rep*. 2017;7(1):6109.
- Li H, Zhang L, Li J, Wu Q, Qian L, He J, et al. Resistant starch intake facilitates weight loss in humans by reshaping the gut microbiota. *Nat Metab*. 2024;6(3):578–97.
- Roager HM, Licht TR. Microbial tryptophan catabolites in health and disease. *Nat Commun*. 2018;9(1):3294.
- Gardner CD, Trepanowski JF, Del Gobbo LC, Hauser ME, Rigdon J, Ioannidis JP, et al. Effect of low-fat vs low-carbohydrate diet on 12-month weight loss in overweight adults and the association with genotype pattern or insulin secretion: the DIETFITS randomized clinical trial. *JAMA*. 2018;319(7):667–79.
- Aguirre M, Ramiro-García J, Koenen ME, Venema K. To pool or not to pool? Impact of the use of individual and pooled fecal samples for in vitro fermentation studies. *J Microbiol Meth*. 2014;107:1–7.
- Kolodziejczyk AA, Zheng D, Elinav E. Diet-microbiota interactions and personalized nutrition. *Nat Rev Microbiol*. 2019;17(12):742–53.
- Brodkorb A, Egger L, Alminger M, Alvioto P, Assunção R, Ballance S, et al. INFOGEST static in vitro simulation of gastrointestinal food digestion. *Nat Protoc*. 2019;14(4):991–1014.
- O'Donnell MM, Rea MC, Shanahan F, Ross RP. The use of a mini-bioreactor fermentation system as a reproducible, high-throughput ex vivo batch model of the distal colon. *Front Microbiol*. 2018;9:1844.
- Verney J, Schwartz C, Amiche S, Pereira B, Thivel D. Comparisons of a multi-frequency bioelectrical impedance analysis to the dual-energy X-ray absorptiometry scan in healthy young adults depending on their physical activity level. *J Hum Kinet*. 2015;47(1):73–80.
- Kyle UG, Bosaeus I, De Lorenzo AD, Deurenberg P, Elia M, Gómez JM, et al. Bioelectrical impedance analysis—part II: utilization in clinical practice. *Clin Nutr*. 2004;23(6):1430–53.
- Authority EFS. General principles for the collection of national food consumption data in the view of a pan-European dietary survey. *EFSA J*. 2009;7(12):1435.
- Brussaard J, Löwik M, Steingrimsdóttir L, Möller A, Kearney J, De Henauw S, et al. A European food survey methodology—conclusions and recommendations. *Eur J Clin Nutr*. 2002;56(2):S89–94.
- Ortega RM, López-Sobaler AM, Andrés P, Rodríguez-Rodríguez E, Aparicio A, Bermejo LM. Increasing consumption of breakfast cereal improves thiamine status in overweight/obese women following a hypocaloric diet. *Int J Food Sci Nutr*. 2009;60(1):69–79.
- Pérez-Burillo S, Molino S, Navajas-Porras B, Valverde-Moya AJ, Hinojosa-Nogueira D, López-Maldonado A, et al. An in vitro batch fermentation protocol for studying the contribution of food to gut microbiota composition and functionality. *Nat Protoc*. 2021;16(7):3186–209.
- Lotti C, Rubert J, Fava F, Tuohy K, Mattivi F, Vrhovsek U. Development of a fast and cost-effective gas chromatography-mass spectrometry method for the quantification of short-chain and medium-chain fatty acids in human biofluids. *Anal Bioanal Chem*. 2017;409:5555–67.
- Huang Z, de Vries S, Fogliano V, Wells JM, van der Wielen N, Capuano E. Effect of whole foods on the microbial production of tryptophan-derived aryl hydrocarbon receptor agonists in growing pigs. *Food Chem*. 2023;416:135804.

38. Bushnell B. BMap: BMap short read aligner, and other bioinformatic tools. 2014. <https://sourceforge.net/projects/bbmap/>. Accessed 15 Oct 2022.
39. Coelho LP, Alves R, Monteiro P, Huerta-Cepas J, Freitas AT, Bork P. NG-meta-profiler: fast processing of metagenomes using NGLess, a domain-specific language. *Microbiome*. 2019;7(1):1–10.
40. McIver LJ, Abu-Ali G, Franzosa EA, Schwager R, Morgan XC, Waldron L, et al. bioBakery: a meta'omic analysis environment. *Bioinformatics*. 2018;34(7):1235–7.
41. Beghini F, McIver LJ, Blanco-Míguez A, Dubois L, Asnicar F, Maharjan S, et al. Integrating taxonomic, functional, and strain-level profiling of diverse microbial communities with bioBakery 3. *elife*. 2021;10:e65088.
42. Lu Y, Zhou G, Ewald J, Pang Z, Shiri T, Xia J. MicrobiomeAnalyst 2.0: comprehensive statistical, functional and integrative analysis of microbiome data. *Nucleic Acids Res*. 2023;1:51.
43. Mallick H, Rahnavad A, McIver LJ, Ma S, Zhang Y, Nguyen LH, et al. Multivariable association discovery in population-scale meta-omics studies. *PLoS Comput Biol*. 2021;17(11):e1009442.
44. Ritchie ME, Phipson B, Wu D, Hu Y, Law CW, Shi W, et al. limma powers differential expression analyses for RNA-seq and microarray studies. *Nucleic Acids Res*. 2015;43(7):e47–e47.
45. Pascal Andreu V, Roel-Touris J, Dodd D, Fischbach MA, Medema MH. The gutSMASH web server: automated identification of primary metabolic gene clusters from the gut microbiota. *Nucleic Acids Res*. 2021;49(W1):W263–70.
46. Pascal Andreu V, Augustijn HE, Chen L, Zhernakova A, Fu J, Fischbach MA, et al. gutSMASH predicts specialized primary metabolic pathways from the human gut microbiota. *Nat Biotechnol*. 2023;41(10):1416–23.
47. Zimmermann J, Kaleta C, Waschina S. gapseq: Informed prediction of bacterial metabolic pathways and reconstruction of accurate metabolic models. *Genome Biol*. 2021;22(1):1–35.
48. Bauer E, Zimmermann J, Baldini F, Thiele I, Kaleta C. BacArena: Individual-based metabolic modeling of heterogeneous microbes in complex communities. *PLoS Comput Biol*. 2017;13(5):e1005544.
49. Magnúsdóttir S, Heinken A, Kutt L, Ravcheev DA, Bauer E, Noronha A, et al. Generation of genome-scale metabolic reconstructions for 773 members of the human gut microbiota. *Nat Biotechnol*. 2017;35(1):81–9.
50. Index WBM. BMIANTHROPOMETRY. 2017. <https://apps.who.int/gho/data/node.main>. Accessed 10 Nov 2022.
51. Liu Y, Chen H, Van Treuren W, Hou BH, Higginbottom SK, Dodd D. *Clostridium sporogenes* uses reductive Stickland metabolism in the gut to generate ATP and produce circulating metabolites. *Nat Microbiol*. 2022;7(5):695–706.
52. Kasai C, Sugimoto K, Moritani I, Tanaka J, Oya Y, Inoue H, et al. Comparison of the gut microbiota composition between obese and non-obese individuals in a Japanese population, as analyzed by terminal restriction fragment length polymorphism and next-generation sequencing. *BMC Gastroenterol*. 2015;15:1–10.
53. Miquel S, Martín R, Bridonneau C, Robert V, Sokol H, Bermúdez-Humarán LG, et al. Ecology and metabolism of the beneficial intestinal commensal bacterium *Faecalibacterium prausnitzii*. *Gut Microbes*. 2014;5(2):146–51.
54. Maioli TU, Borrás-Nogues E, Torres L, Barbosa SC, Martins VD, Langella P, et al. Possible benefits of *Faecalibacterium prausnitzii* for obesity-associated gut disorders. *Front Pharmacol*. 2021;12:740636.
55. Zhang X, Shen D, Fang Z, Jie Z, Qiu X, Zhang C, et al. Human gut microbiota changes reveal the progression of glucose intolerance. *PLoS ONE*. 2013;8(8):e71108.
56. Turnbaugh PJ, Ley RE, Mahowald MA, Magrini V, Mardis ER, Gordon JL. An obesity-associated gut microbiome with increased capacity for energy harvest. *Nature*. 2006;444(7122):1027–31.
57. Magne F, Gotteland M, Gauthier L, Zazueta A, Pessoa S, Navarrete P, et al. The firmicutes/bacteroidetes ratio: a relevant marker of gut dysbiosis in obese patients? *Nutrients*. 2020;12(5):1474.
58. Kallus SJ, Brandt LJ. The intestinal microbiota and obesity. *J Clin Gastroenterol*. 2012;46(1):16–24.
59. Tiihonen K, Ouwehand AC, Rautonen N. Effect of overweight on gastrointestinal microbiology and immunology: correlation with blood biomarkers. *Br J Nutr*. 2010;103(7):1070–8.
60. Daniel N, Nachbar RT, Tran TTT, Ouellette A, Varin TV, Cotillard A, et al. Gut microbiota and fermentation-derived branched chain hydroxy acids mediate health benefits of yogurt consumption in obese mice. *Nat Commun*. 2022;13(1):1343.
61. Watson E, MacNeil LT, Ritter AD, Yilmaz LS, Rosebrock AP, Caudy AA, et al. Interspecies systems biology uncovers metabolites affecting *C. elegans* gene expression and life history traits. *Cell*. 2014;156(4):759–70.
62. Saad M, Santos A, Prada P. Linking gut microbiota and inflammation to obesity and insulin resistance. *Physiology*. 2016;31(4):283–93.
63. Pedersen HK, Gudmundsdóttir V, Nielsen HB, Hyötyläinen T, Nielsen T, Jensen BA, et al. Human gut microbes impact host serum metabolome and insulin sensitivity. *Nature*. 2016;535(7612):376–81.
64. Ridaura VK, Faith JJ, Rey FE, Cheng J, Duncan AE, Kau AL, et al. Gut microbiota from twins discordant for obesity modulate metabolism in mice. *Science*. 2013;341(6150):1241214.
65. Choi BSY, Daniel N, Houde VP, Ouellette A, Marcotte B, Varin TV, et al. Feeding diversified protein sources exacerbates hepatic insulin resistance via increased gut microbial branched-chain fatty acids and mTORC1 signaling in obese mice. *Nat Commun*. 2021;12(1):3377.
66. Wu M, McNulty NP, Rodionov DA, Khoroshkin MS, Griffin NW, Cheng J, et al. Genetic determinants of in vivo fitness and diet responsiveness in multiple human gut *Bacteroides*. *Science*. 2015;350(6256):aac5992.
67. McCann JR, Rawls JF. Essential amino acid metabolites as chemical mediators of host-microbe interaction in the Gut. *Annu Rev Microbiol*. 2023;77:479–97.
68. Dodd D, Spitzer MH, Van Treuren W, Merrill BD, Hryckowian AJ, Higginbottom SK, et al. A gut bacterial pathway metabolizes aromatic amino acids into nine circulating metabolites. *Nature*. 2017;551(7682):648–52.
69. Rios-Covian D, González S, Nogačka AM, Arboleya S, Salazar N, Gueimonde M, et al. An overview on fecal branched short-chain fatty acids along human life and as related with body mass index: associated dietary and anthropometric factors. *Front Microbiol*. 2020;11:513909.
70. Saresella M, Marventano I, Barone M, La Rosa F, Piancone F, Mendozzi L, et al. Alterations in circulating fatty acid are associated with gut microbiota dysbiosis and inflammation in multiple sclerosis. *Front Immunol*. 2020;11:1390.
71. Zhu X, Zhou Y, Wang Y, Wu T, Li X, Li D, et al. Production of high-concentration n-caproic acid from lactate through fermentation using a newly isolated Ruminococcaceae bacterium CPB6. *Biotechnol Biofuels*. 2017;10:1–12.
72. Scarborough MJ, Lawson CE, Hamilton JJ, Donohue TJ, Noguera DR. Metatranscriptomic and thermodynamic insights into medium-chain fatty acid production using an anaerobic microbiome. *MSystems*. 2018;3(6):e00221-18.
73. Yassour M, Lim MY, Yun HS, Tickle TL, Sung J, Song YM, et al. Sub-clinical detection of gut microbial biomarkers of obesity and type 2 diabetes. *Genome Med*. 2016;8:1–14.
74. Brahe LK, Le Chatelier E, Prifti E, Pons N, Kennedy S, Hansen T, et al. Specific gut microbiota features and metabolic markers in postmenopausal women with obesity. *Nutr Diabetes*. 2015;5(6):e159–e159.
75. Liu R, Hong J, Xu X, Feng Q, Zhang D, Gu Y, et al. Gut microbiome and serum metabolome alterations in obesity and after weight-loss intervention. *Nat Med*. 2017;23(7):859–68.
76. Dao MC, Everard A, Aron-Wisnewsky J, Sokolovska N, Prifti E, Verger EO, et al. *Akkermansia muciniphila* and improved metabolic health during a dietary intervention in obesity: relationship with gut microbiome richness and ecology. *Gut*. 2016;65(3):426–36.
77. Kschonsek J, Wolfram T, Stöckl A, Böhm V. Polyphenolic compounds analysis of old and new apple cultivars and contribution of polyphenolic profile to the in vitro antioxidant capacity. *Antioxidants*. 2018;7(1):20.
78. Shahidi F, Yeo J. Insoluble-bound phenolics in food. *Molecules*. 2016;21(9):1216.
79. Lupa B, Lyon D, Gibbs MD, Reeves RA, Wiegel J. Distribution of genes encoding the microbial non-oxidative reversible hydroxyarylic acid decarboxylases/phenol carboxylases. *Genomics*. 2005;86(3):342–51.
80. Yoda Y, Hu ZQ, Shimamura T, Zhao WH. Different susceptibilities of *Staphylococcus* and Gram-negative rods to epigallocatechin gallate. *J Infect Chemother*. 2004;10(1):55–8.
81. Schellekens H, Torres-Fuentes C, van de Wouw M, Long-Smith CM, Mitchell A, Strain C, et al. *Bifidobacterium longum* counters the effects of

- obesity: partial successful translation from rodent to human. *EBioMedicine*. 2021;63.
82. Wang G, Fan Y, Zhang G, Cai S, Ma Y, Yang L, et al. Microbiota-derived indoles alleviate intestinal inflammation and modulate microbiome by microbial cross-feeding. *Microbiome*. 2024;12(1):59.
  83. Sinha AK, Laursen MF, Brinck JE, Rybtke ML, Hjørne AP, Procházková N, et al. Dietary fibre directs microbial tryptophan metabolism via metabolic interactions in the gut microbiota. *Nat Microbiol*. 2024. <https://doi.org/10.1038/s41564-024-01737-3>.
  84. Arnoriaga-Rodríguez M, Mayneris-Perxachs J, Burokas A, Contreras-Rodríguez O, Blasco G, Coll C, et al. Obesity impairs short-term and working memory through gut microbial metabolism of aromatic amino acids. *Cell Metab*. 2020;32(4):548–60.
  85. Collins SM, Surette M, Bercik P. The interplay between the intestinal microbiota and the brain. *Nat Rev Microbiol*. 2012;10(11):735–42.
  86. Zhao S, Lau R, Zhong Y, Chen MH. Lactate cross-feeding between *Bifidobacterium* species and *Megasphaera indica* contributes to butyrate formation in the human colonic environment. *Appl Environ Microbiol*. 2023;90.
  87. Nagara Y, Fujii D, Takada T, Sato-Yamazaki M, Odani T, Oishi K. Selective induction of human gut-associated acetogenic/butyrogenic microbiota based on specific microbial colonization of indigestible starch granules. *ISME J*. 2022;16(6):1502–11.

### **Publisher's Note**

Springer Nature remains neutral with regard to jurisdictional claims in published maps and institutional affiliations.